Supporting Information for:

Validating the Biphilic Hypothesis of Nontrigonal P(III) Compounds

Kyounghoon Lee,[‡#] Anastasia V. Blake,[‡#] Akira Tanushi,[†] Sean M. McCarthy,[§] Daniel Kim,[⊥] Sydney M. Loria,[⊥] Courtney M. Donahue,[‡] Kyle D. Spielvogel,[‡] Jason M. Keith,[*⊥] Scott R. Daly,[*‡] Alexander T. Radosevich[*†]

[†]*Department of Chemistry, Massachusetts Institute of Technology, Cambridge, Massachusetts 02139, United States*

[‡]*Department of Chemistry, The University of Iowa, E331 Chemistry Building, Iowa City, Iowa 52242-1294, United States*

[§]*Nalas Engineering Services, Inc., 85 Westbrook Rd., Centerbook, Connecticut 06409*

[⊥]*Department of Chemistry, Colgate University, 13 Oak Drive, Hamilton, New York 13346, United States*

[#]*These authors contributed equally to this work.*

CONTENTS

I. General Methods.

All reagents were purchased from commercial vendors and used as received unless otherwise noted. Diethyl ether (Et$_2$O), methylene chloride (CH$_2$Cl$_2$), tetrahydrofuran (THF), and pentane were dried according to the method of Grubbs[1] as modified by Bergman[2] using a Glass Contour Solvent Purification System. All glassware was oven-dried at 120 °C prior to use. All reactions were carried out under dry nitrogen atmosphere (Schlenk line or glovebox) unless otherwise noted. Solution NMR spectra were recorded on a VARIAN Inova-500 (500 MHz) spectrometer and processed with a MestReNova software. ^{1}H NMR chemical shifts (δ in ppm) were calibrated to the residual solvent peak (C$_6$D$_6$, δ 7.16 ppm). ^{13}C$\{^{1}$H$\}$ NMR shifts are given in ppm with respect to solvent residual peak (C$_6$D$_6$, δ 128.06 ppm). Coupling constants are reported as *J*-values in Hz. High resolution ESI mass spectra were obtained from the Mass Spectrometry Laboratory at the School of Chemical Sciences, University of Illinois at Urbana-Champaign. X-ray diffraction data was collected on a Bruker SMART APEX CCD area detector system equipped with a graphite monochromator and a MoKα fine-focus sealed tube (λ = 0.71073 Å). Raw data integration and reduction were performed with the SAINT[3] and SADABS[4] programs. Structures were solved by direct methods using SHELXT[5] and refined by least-squares methods on F^2 using the SHELXL software package. All non-hydrogen atoms were refined with anisotropic displacement parameters. The hydrogen atoms attached to phosphorus were located in Fourier maps and were refined isotropically without constraints. All other hydrogen atoms were fixed in their ideal geometries. Graphical representations were generated in XP.

II. Synthesis and characterization

Compounds P(NMePh)$_3$,[6] **1**,[7] **2**,[8] **2•[Ru]**,[8] and **2•[H][Ru]**[8] were synthesized according to the literature procedures and characterized by ^{1}H and ^{31}P NMR spectroscopy prior to use. The crystal structure of P(NMePh)$_3$ (see Supporting Information Section IV for details) was determined to allow for comparison of its metrical parameters with cyclic analogues.

Synthesis of 1•[H]$_2$. To a solution of **1•[Cl]$_2$**[7] (20 mg, 0.061 mmol) in tetrahydrofuran (5 mL) at –35 °C was added sodium cyanoborohydride (77 mg, 0.12 mmol) in one portion. The reaction mixture was stirred 1 h, then warmed to ambient temperature. The solvent was subsequently removed in vacuo. The solid residue was triturated with pentane, and the suspension was filtered over celite. The colorless filtrate was evaporated to give the product **1•[H]$_2$** as a white solid (13 mg, 80 %). A single crystalline sample of **1•[H]$_2$** was obtained from a concentrated pentane solution at –35°C.

^{1}H NMR (500 MHz, C$_6$D$_6$) δ 7.40 (d, J = 7.6 Hz, 2H), 7.07 (d, J = 523 Hz, 2H), 7.03 – 6.93 (m, 4H), 6.51 (d, J = 7.2 Hz, 2H), 2.44 (d, J = 16.7 Hz, 6H). ^{31}P NMR (203 MHz, C$_6$D$_6$) δ –67.7 (triplet of septets, J = 523, 16.6 Hz). ^{13}C NMR (126 MHz, C$_6$D$_6$) δ 133.9 (d, J = 13.1 Hz), 131.8 (d, J = 14.6 Hz), 120.5, 119.8, 110.6 (d, J = 9.2 Hz), 108.7 (d, J = 7.2 Hz), 28.1 (d, J = 14.9 Hz). MS (ESI) calc'd for C$_{14}$H$_{16}$N$_3$P (M+): 257.1082, found: 257.1078.

Although multinuclear NMR spectroscopy suggested an apparent C_{2v} symmetry of **1•[H]$_2$** in solution, X-ray diffraction of a colorless single crystal of **1•[H]$_2$** gives evidence for a solid state structure of approximate C_s symmetry. The geometry about the pentacoordinate phosphorus may be described as quasi-square pyramidal (τ_5 = 0.33),[9] where the two hydride ligands occupy inequivalent apical and basal positions (∠H$_1$–P–N$_2$ = 98.3° and ∠H$_2$–P– N$_2$ = 165.7°) and the chelating triamide binds at the remaining basal vacancies. The apparent discrepancy between the solution and solid state structures for **1•[H]$_2$** can be rationalized by reference to DFT calculations (B3LYP/6-31G**), which indicate a low energy C_{2v} symmetric saddle point (E_{rel} = 5.8 kcal/mol) along the PH2 rocking coordinate connecting degenerate C_s symmetric minima for **1•[H]$_2$**, consistent with rapid interconversion and time-averaging on the NMR timescale.

III. Phosphorus K-edge XANES Methods and Data.

Overview. Phosphorus K-edge X-ray absorption near-edge structure spectroscopy (XANES) is an element-specific technique that allows for direct measurement of unoccupied frontier orbital composition and energy by probing dipole-allowed transitions from the core P 1s → empty orbitals containing phosphorus p character.[10-11] As such, phosphorus K-edge XANES is an ideal tool for extracting valuable information concerning electronic structure and chemical bonding in phosphorus compounds of diverse structure and composition.[12] For example, Szilagyi in collaboration with Peters and Mindiola used phosphorus K-edge XANES to help elucidate redox and magnetic contributions to electronic structure in metal diphosphine and pincer complexes.[13-16] More recent efforts by Daly and Keith used phosphorus K-edge XANES to determine how structural changes in phosphorus ligands give rise to relative differences in metal-phosphorus covalency.[-20]

XANES Sample Preparation. P K-edge XANES samples were prepared in an N_2-filled glovebox with <1.0 ppm O_2 by grinding crystalline $P(NMePh)_3$, **1**, **1•[H]$_2$**, **2•[Ru]**, and **2•[H][Ru]** (ca. 10 mg) for 2 min using a Wig-L-Bug grinder and polystyrene capsules containing a Plexiglas pestle. The resulting powder for **1** and **1•[H]$_2$** was dusted onto single-sided tape (40 μm) exposed through a 5 x 20 x 1 mm window on an aluminum plate using a series 237 Winsor & Newton University Bright brush. P K-edge XANES analysis of the tape, brush fibers, and Wig-L-Bug materials confirmed them to have no measurable phosphorus impurities. The samples were sealed behind two layers of polypropylene film (4 μm, SPEX CertiPrep) separated by an aluminum spacer (1 μM) and transported to the beamline in a sealed container under N_2. The container was placed in a glovebag attached to the He-filled sample chamber, and the samples were quickly loaded into the sample chamber after the glovebag had purged for 30 minutes with inert gas (N_2 or He). Samples of $P(NMePh)_3$, **2•[Ru]**, and **2•[H][Ru]** were prepared similarly, but their data were first collected using a gas-flow cell designed at Iowa for air-sensitive XAS measurements in the tender X-ray region.[20] Subsequent P K-edge XANES data collected on **2•[Ru]** and **2•[H][Ru]** after brief exposure to air revealed no differences when compared to samples handled under rigorously air-free conditions.

XANES Data Collection and Analysis. All P K-edge XANES data were collected as previously described on BL 14-3 at the Stanford Synchrotron Radiation Lightsource (SSRL) in Menlo Park, CA under dedicated operating conditions of 3.0 GeV and 500 mA.[17,2021-23] BL 14-3 is equipped with a bending magnet source and a water-cooled double crystal Si(111) monochromator. The sample chamber and gas-flow cell (when used) were maintained under a slow purge of He during data collection. Data were collected in fluorescence mode using a PIPS detector in triplicate sets for each sample over three energy regions, as described previously.[20] The step sizes over the pre-edge (~2106-2140 eV), edge (~2140-2180 eV), and post-edge (~2180-2380 eV) were 1.0, 0.08, and 1.5 eV, respectively. A calibration scan was collected before and after each set of scans on $Na_4P_2O_7$ (2152.40 eV) or PPh_4Br (2146.96 eV).[24] Calibrations, background subtraction, normalization, and averaging of individual scans were completed using the Athena program in the

IFFEFIT XAS software package.[25] A first order polynomial was fit to the pre-edge region to remove the background from each scan. The background-subtracted scans were normalized by fitting a second or third order polynomial to the post-edge regions and setting the step function to an intensity of 1.0 at a set point of 2165 eV.
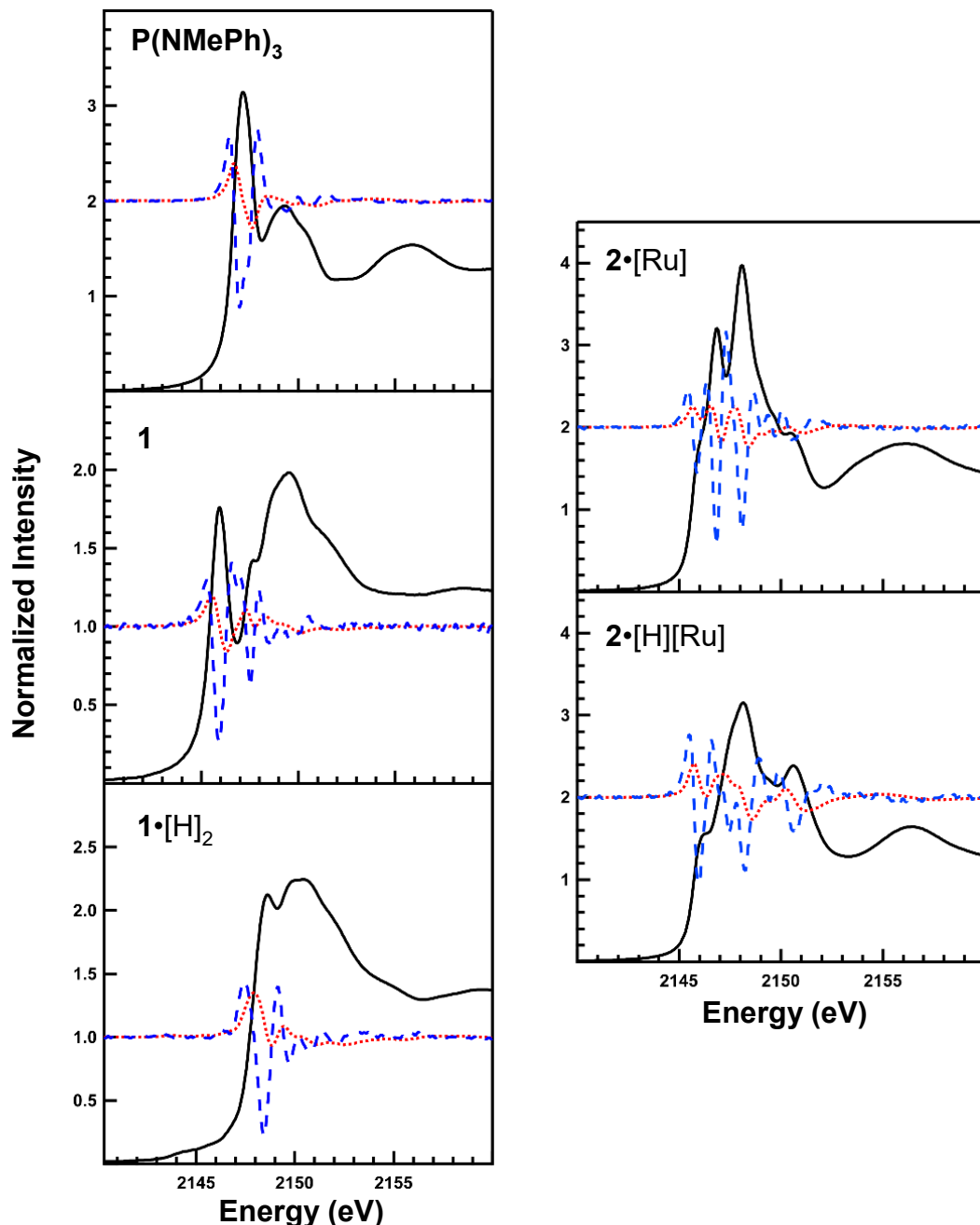
Figure S1. Comparison of P K-edge XANES spectra for P(NMePh)$_3$, **1**, and **1**•[H]$_2$ (*left*) and **2**•[Ru], and **2**•[H][Ru] (*right*). First (red; dotted line) and second (blue; dashed line) derivatives divided by 5 or 10 are offset on the y-axis by +1 or +2 intensity units.
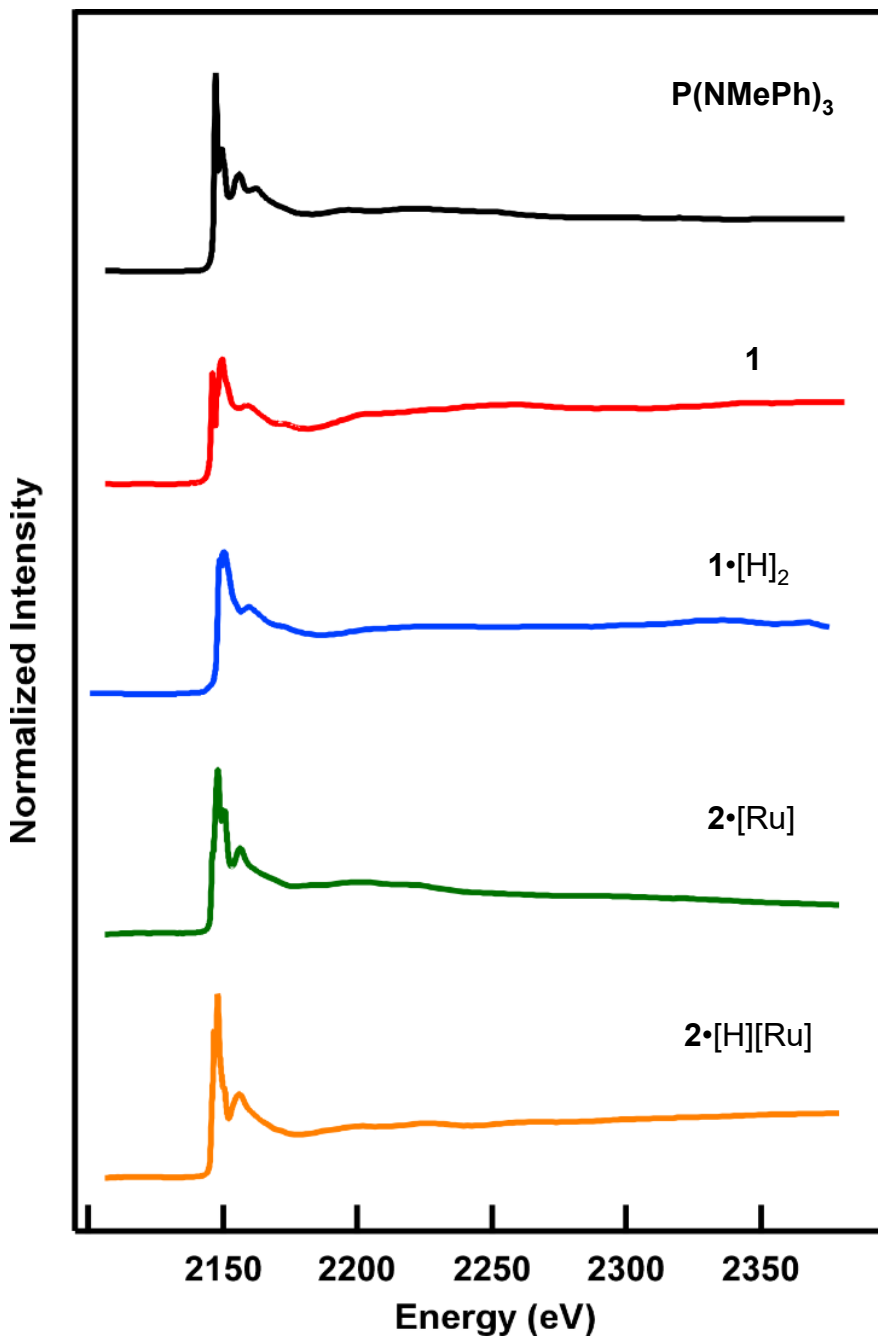
Figure S2. Complete background-subtracted and normalized P K-edge XANES spectra of P(NMePh)$_3$, **1**, **1**•[H]$_2$, **2**•[Ru], and **2**•[H][Ru].

IV. Crystallographic Data

Table S1. Selected Bond Distances (Å) and Angles (°) for P(NMePh)$_3$, **1**, **1**•[H]$_2$, **2**, **2**•[Ru], and **2**•[H][Ru].

metric	P(NMePh)$_3$	**1**[a]	**1**•[H]$_2$	**2**[b]	**2**•[Ru][b]	**2**•[H][Ru][b]
$d(Ru_1–P_1)$					2.1262(3)	2.2509(4)
$d(Ru_1–P_2)$					2.3329(3)	2.3359(4)
$d(P_1–N_1)$	1.7193(19)	1.7610(12)	1.7879(9)	1.7485(8)	1.7085(9)	1.7178(14)
$d(P_1–N_2)$	1.7193(19)	1.7190(13)	1.7098 (10)	1.7341(8)	1.7280(9)	1.8362(14)
$d(P_1–N_3)$	1.7193(19)	1.7014(14)	1.7088(9)	1.7786(8)	1.7135(9)	1.8193(15)
$∠Ru_1–P_1–N_1$					147.62(3)	140.14(6)
$∠N_2–P_1–N_3$	101.33(9)	115.21(7)	146.00	108.67(4)	113.94(4)	170.74(7)
$∠N_1–P_1–N_2$	101.33(9)	90.08(6)	86.14	90.56(4)	91.40(4)	86.59(7)
$∠N_1–P_1–N_3$	101.33(9)	90.51(6)	86.32	89.45(4)	92.04(4)	87.25(7)

[a] Data from Ref. 7.

[b] Data from Ref. 8.
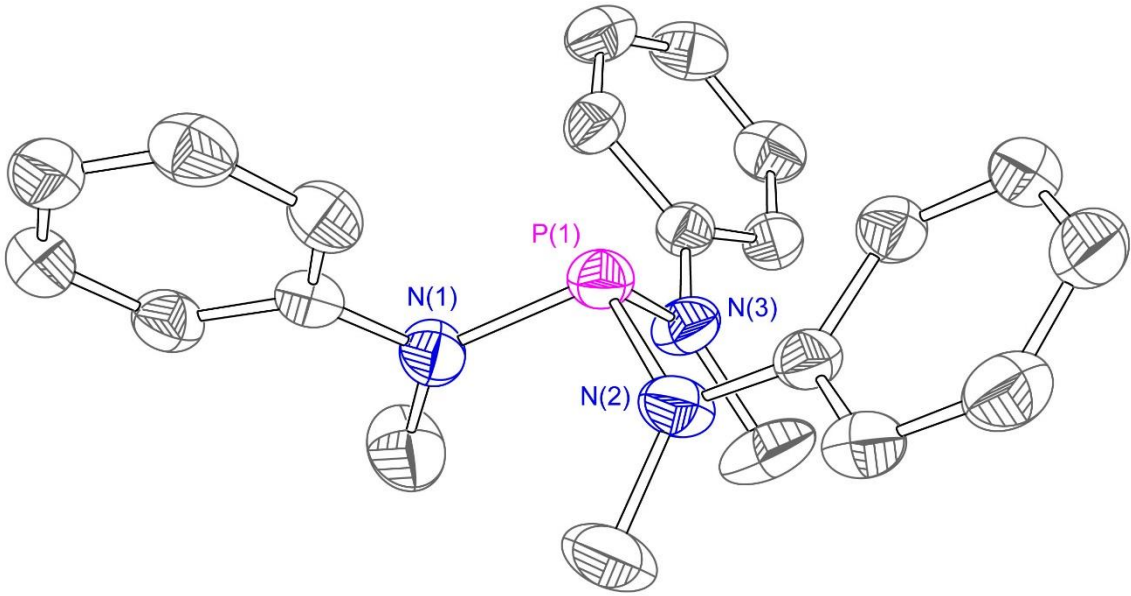
Figure S3. Solid-state structure of P(NMePh)$_3$. Thermal ellipsoid plots rendered at the 50% probability level.

The X-ray structure of P(NMePh)$_3$ confirmed the *C$_3$* symmetric structure, where the angles (∠N–P–N = 101.3°) and distances (*d*(P–N)=1.719 Å) are all equivalent in the primary bonding environment of phosphorus. The *N*-aryl moieties are displayed in all-*syn* helical fashion proximal to the phosphorus lone pair, with the less sterically demanding methyl substituents on the concave face of the trigonal pyramid.[26]

Table S2. Crystal data and structure refinement for P(NMePh)$_3$.

Identification code	smm8r
Empirical formula	C21 H24 N3 P
Formula weight	349.40
Temperature	199(2) K
Wavelength	0.71073 Å
Crystal system	Rhombohedral
Space group	R3
Unit cell dimensions	a = 12.724(3) Å α= 90°.
	b = 12.724(3) Å β= 90°.
	c = 9.994(4) Å γ = 120°.
Volume	1401.3(7) Å^3
Z	3
Density (calculated)	1.242 Mg/m^3
Absorption coefficient	0.155 mm^{-1}
F(000)	558
Crystal size	0.23 x 0.22 x 0.16 mm^3
Theta range for data collection	2.75 to 28.25°.
Index ranges	-15<=h<=16, -16<=k<=14, -8<=l<=13
Reflections collected	2382
Independent reflections	991 [R(int) = 0.0291]
Completeness to theta = 28.25°	99.1 %
Absorption correction	Semi-empirical from equivalents
Max. and min. transmission	0.9756 and 0.9652
Refinement method	Full-matrix least-squares on F^2
Data / restraints / parameters	991 / 1 / 77
Goodness-of-fit on F^2	1.145
Final R indices [I>2sigma(I)]	R1 = 0.0348, wR2 = 0.1010
R indices (all data)	R1 = 0.0352, wR2 = 0.1015
Absolute structure parameter	0.40(14)
Largest diff. peak and hole	0.187 and -0.233 e.Å^{-3}

Table S3. Atomic coordinates (x 10^4) and equivalent isotropic displacement parameters (Å^2x 10^3) for P(NMePh)$_3$. U(eq) is defined as one third of the trace of the orthogonalized U^{ij} tensor.

	x	y	z	U(eq)
C(1)	8987(2)	7586(2)	8915(2)	34(1)
C(2)	8186(2)	7523(2)	7921(2)	40(1)
C(3)	7466(2)	6452(2)	7241(3)	48(1)
C(4)	7495(2)	5411(2)	7562(3)	51(1)
C(5)	8250(3)	5452(2)	8577(3)	49(1)
C(6)	8994(2)	6520(2)	9248(2)	41(1)
C(7)	10408(3)	8660(3)	10751(3)	65(1)
N(1)	9759(2)	8691(2)	9563(2)	40(1)
P(1)	10000	10000	8790(1)	36(1)

Table S4. Bond lengths [Å] and angles [°] for P(NMePh)₃.

_____

C(1)-C(2)	1.396(3)
C(1)-C(6)	1.401(3)
C(1)-N(1)	1.408(3)
C(2)-C(3)	1.382(3)
C(2)-H(2)	0.9300
C(3)-C(4)	1.381(4)
C(3)-H(3)	0.9300
C(4)-C(5)	1.380(4)
C(4)-H(4)	0.9300
C(5)-C(6)	1.381(4)
C(5)-H(5)	0.9300
C(6)-H(6)	0.9300
C(7)-N(1)	1.458(3)
C(7)-H(7A)	0.9600
C(7)-H(7B)	0.9600
C(7)-H(7C)	0.9600
N(1)-P(1)	1.7193(19)
P(1)-N(1)#1	1.7193(19)
P(1)-N(1)#2	1.7193(19)
C(2)-C(1)-C(6)	118.1(2)
C(2)-C(1)-N(1)	120.64(19)
C(6)-C(1)-N(1)	121.24(19)
C(3)-C(2)-C(1)	120.7(2)
C(3)-C(2)-H(2)	119.6
C(1)-C(2)-H(2)	119.6
C(4)-C(3)-C(2)	120.6(2)
C(4)-C(3)-H(3)	119.7
C(2)-C(3)-H(3)	119.7
C(5)-C(4)-C(3)	119.2(2)
C(5)-C(4)-H(4)	120.4
C(3)-C(4)-H(4)	120.4
C(4)-C(5)-C(6)	121.0(2)
C(4)-C(5)-H(5)	119.5

C(6)-C(5)-H(5)	119.5
C(5)-C(6)-C(1)	120.3(2)
C(5)-C(6)-H(6)	119.8
C(1)-C(6)-H(6)	119.8
N(1)-C(7)-H(7A)	109.5
N(1)-C(7)-H(7B)	109.5
H(7A)-C(7)-H(7B)	109.5
N(1)-C(7)-H(7C)	109.5
H(7A)-C(7)-H(7C)	109.5
H(7B)-C(7)-H(7C)	109.5
C(1)-N(1)-C(7)	118.0(2)
C(1)-N(1)-P(1)	117.24(15)
C(7)-N(1)-P(1)	124.33(17)
N(1)#1-P(1)-N(1)	101.33(9)
N(1)#1-P(1)-N(1)#2	101.33(9)
N(1)-P(1)-N(1)#2	101.33(9)

_____

Symmetry transformations used to generate equivalent atoms:

#1 -y+2,x-y+1,z   #2 -x+y+1,-x+2,z

Table S5. Anisotropic displacement Å^{2}x 10^3) for P(NMePh)$_3$. The anisotropic displacement factor exponent takes the form: $-2\pi^2[h^2 a^{*2}U^{11} + ... + 2 h k a^* b^* U^{12}]$

	U^{11}	U^{22}	U^{33}	U^{23}	U^{13}	U^{12}
C(1)	34(1)	41(1)	28(1)	4(1)	3(1)	18(1)
C(2)	37(1)	44(1)	38(1)	6(1)	-2(1)	20(1)
C(3)	40(1)	55(1)	36(1)	3(1)	-5(1)	15(1)
C(4)	55(1)	42(1)	40(1)	-1(1)	4(1)	13(1)
C(5)	62(1)	41(1)	42(1)	6(1)	7(1)	25(1)
C(6)	47(1)	48(1)	33(1)	6(1)	2(1)	27(1)
C(7)	82(2)	58(2)	48(2)	-1(1)	-31(1)	30(1)
N(1)	49(1)	41(1)	34(1)	0(1)	-9(1)	24(1)
P(1)	39(1)	39(1)	30(1)	0	0	20(1)

Table S6. Hydrogen coordinates (x 10^4) and isotropic displacement parameters ($Å^2$x 10^3) for P(NMePh)$_3$.

	x	y	z	U(eq)
H(2)	8137	8210	7714	48
H(3)	6958	6432	6560	57
H(4)	7011	4692	7101	61
H(5)	8259	4749	8811	59
H(6)	9501	6532	9925	49
H(7A)	9837	8120	11400	98
H(7B)	10860	9460	11124	98
H(7C)	10956	8377	10510	98

Table S7. Torsion angles [°] for P(NMePh)₃.

C(6)-C(1)-C(2)-C(3)	-3.2(3)
N(1)-C(1)-C(2)-C(3)	177.1(2)
C(1)-C(2)-C(3)-C(4)	2.2(4)
C(2)-C(3)-C(4)-C(5)	0.2(4)
C(3)-C(4)-C(5)-C(6)	-1.5(4)
C(4)-C(5)-C(6)-C(1)	0.5(4)
C(2)-C(1)-C(6)-C(5)	1.9(3)
N(1)-C(1)-C(6)-C(5)	-178.4(2)
C(2)-C(1)-N(1)-C(7)	168.9(2)
C(6)-C(1)-N(1)-C(7)	-10.8(3)
C(2)-C(1)-N(1)-P(1)	-18.2(3)
C(6)-C(1)-N(1)-P(1)	162.06(16)
C(1)-N(1)-P(1)-N(1)#1	-160.85(16)
C(7)-N(1)-P(1)-N(1)#1	11.5(3)
C(1)-N(1)-P(1)-N(1)#2	95.0(2)
C(7)-N(1)-P(1)-N(1)#2	-92.6(2)

Symmetry transformations used to generate equivalent atoms:

#1 -y+2,x-y+1,z   #2 -x+y+1,-x+2,z
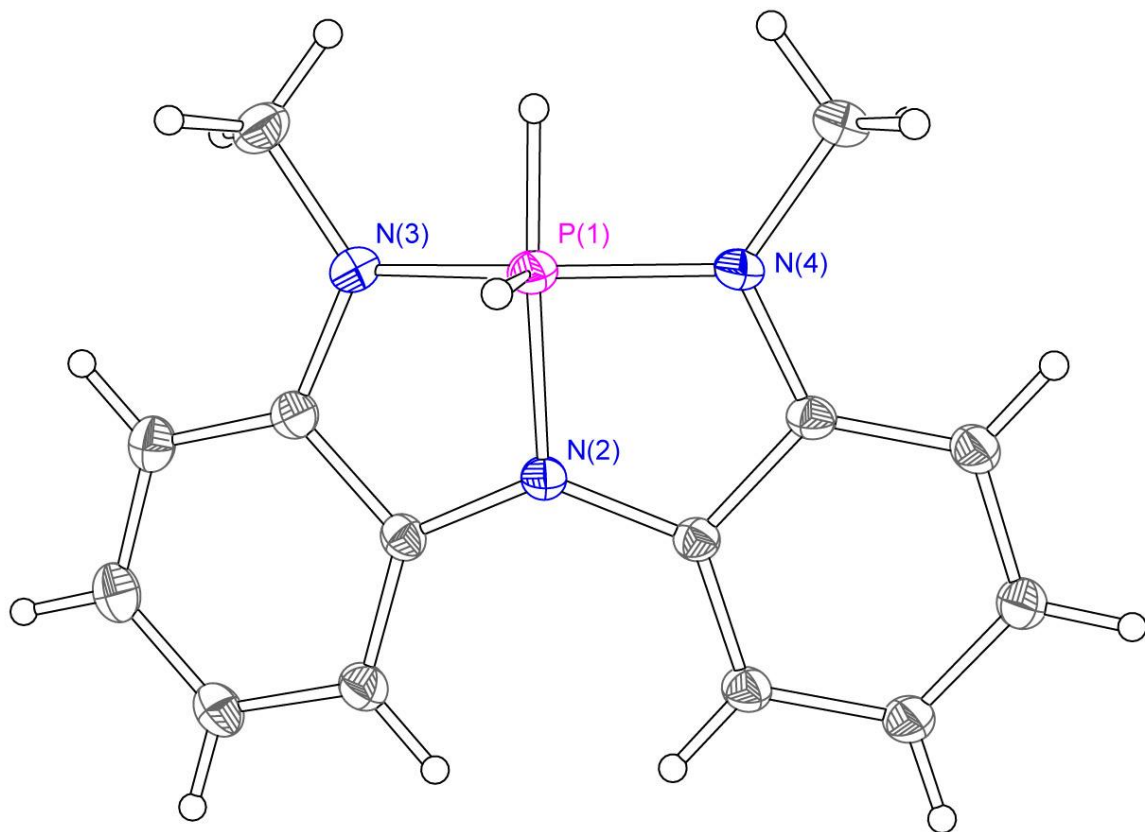
Figure S4. Solid state structure of 1•[H]₂. Thermal ellipsoid plots rendered at the 50% probability level.

Table S8. Crystal data and structure refinement for **1**•[H]$_2$

_____

Identification code	PH2-16
Empirical formula	C14 H16 N3 P
Formula weight	257.27
Temperature	100(2) K
Wavelength	0.71073 Å
Crystal system	Trigonal
Space group	R-3
Unit cell dimensions	a = 29.7625(13) Å α= 90°.
	b = 29.7625(13) Å β= 90°.
	c = 7.5469(4) Å γ = 120°.
Volume	5789.5(6) Å^3
Z	18
Density (calculated)	1.328 Mg/m^3
Absorption coefficient	0.199 mm^{-1}
F(000)	2448
Crystal size	0.429 x 0.064 x 0.062 mm^3
Theta range for data collection	1.368 to 34.031°.
Index ranges	-46<=h<=46, -46<=k<=46, -11<=l<=11
Reflections collected	104083
Independent reflections	5163 [R(int) = 0.0482]
Completeness to theta = 25.242°	99.9 %
Absorption correction	Semi-empirical from equivalents
Max. and min. transmission	0.7467 and 0.7008
Refinement method	Full-matrix least-squares on F^2
Data / restraints / parameters	5163 / 0 / 171
Goodness-of-fit on F^2	1.054
Final R indices [I>2sigma(I)]	R1 = 0.0373, wR2 = 0.0963
R indices (all data)	R1 = 0.0507, wR2 = 0.1037
Extinction coefficient	n/a
Largest diff. peak and hole	0.525 and -0.299 e.Å^{-3}

_____

Table S9. Atomic coordinates (x 10^4) and equivalent isotropic displacement parameters ($Å^2$x 10^3) for **1**•[H]$_2$. U(eq) is defined as one third of the trace of the orthogonalized U^{ij} tensor.

	x	y	z	U(eq)
P(1)	4084(1)	1721(1)	8760(1)	17(1)
N(2)	4330(1)	1767(1)	6566(1)	17(1)
N(3)	4531(1)	2366(1)	8959(1)	18(1)
N(4)	3496(1)	1271(1)	7912(1)	19(1)
C(5)	4580(1)	2677(1)	10508(1)	23(1)
C(6)	3021(1)	1030(1)	8948(2)	24(1)
C(11)	4777(1)	2232(1)	6179(1)	15(1)
C(12)	5097(1)	2385(1)	4701(1)	18(1)
C(13)	5538(1)	2881(1)	4681(1)	22(1)
C(14)	5658(1)	3217(1)	6103(2)	22(1)
C(15)	5335(1)	3068(1)	7592(1)	20(1)
C(16)	4896(1)	2580(1)	7611(1)	16(1)
C(21)	3998(1)	1370(1)	5433(1)	16(1)
C(22)	4085(1)	1233(1)	3756(1)	20(1)
C(23)	3678(1)	803(1)	2904(2)	22(1)
C(24)	3197(1)	518(1)	3700(2)	23(1)
C(25)	3106(1)	654(1)	5385(2)	21(1)
C(26)	3507(1)	1077(1)	6243(1)	17(1)

Table S10. Bond lengths [Å] and angles [°] for **1•[H]₂**.

_____

P(1)-N(3)	1.7088(9)
P(1)-N(4)	1.7098(10)
P(1)-N(2)	1.7879(9)
N(2)-C(11)	1.3892(13)
N(2)-C(21)	1.3918(13)
N(3)-C(16)	1.3886(12)
N(3)-C(5)	1.4529(13)
N(4)-C(26)	1.3929(13)
N(4)-C(6)	1.4521(13)
C(11)-C(12)	1.3876(13)
C(11)-C(16)	1.4129(13)
C(12)-C(13)	1.4025(15)
C(13)-C(14)	1.3864(15)
C(14)-C(15)	1.3990(15)
C(15)-C(16)	1.3860(14)
C(21)-C(22)	1.3927(14)
C(21)-C(26)	1.4135(14)
C(22)-C(23)	1.4031(15)
C(23)-C(24)	1.3838(16)
C(24)-C(25)	1.4020(16)
C(25)-C(26)	1.3886(15)
N(3)-P(1)-N(4)	146.00(5)
N(3)-P(1)-N(2)	86.32(4)
N(4)-P(1)-N(2)	86.14(4)
C(11)-N(2)-C(21)	129.54(8)
C(11)-N(2)-P(1)	114.98(7)
C(21)-N(2)-P(1)	114.51(7)
C(16)-N(3)-C(5)	119.33(9)
C(16)-N(3)-P(1)	116.27(7)
C(5)-N(3)-P(1)	124.07(7)
C(26)-N(4)-C(6)	120.05(9)
C(26)-N(4)-P(1)	115.85(7)
C(6)-N(4)-P(1)	123.20(8)

C(12)-C(11)-N(2)	130.79(9)
C(12)-C(11)-C(16)	119.72(9)
N(2)-C(11)-C(16)	109.49(8)
C(11)-C(12)-C(13)	118.77(9)
C(14)-C(13)-C(12)	121.26(10)
C(13)-C(14)-C(15)	120.33(10)
C(16)-C(15)-C(14)	118.62(9)
C(15)-C(16)-N(3)	126.91(9)
C(15)-C(16)-C(11)	121.28(9)
N(3)-C(16)-C(11)	111.81(9)
N(2)-C(21)-C(22)	130.54(9)
N(2)-C(21)-C(26)	109.47(8)
C(22)-C(21)-C(26)	119.99(9)
C(21)-C(22)-C(23)	118.72(10)
C(24)-C(23)-C(22)	121.16(10)
C(23)-C(24)-C(25)	120.51(10)
C(26)-C(25)-C(24)	118.79(10)
C(25)-C(26)-N(4)	127.60(10)
C(25)-C(26)-C(21)	120.84(9)
N(4)-C(26)-C(21)	111.55(9)

_____

Symmetry transformations used to generate equivalent atoms:

Table S11. Anisotropic displacement parameters $(\text{Å}^2 \text{x } 10^3)$ for **1**•[H]$_2$. The anisotropic displacement factor exponent takes the form: $-2\pi^2[\, h^2\, a^{*2}U^{11} + ... \; + 2\, h\, k\, a^*\, b^*\, U^{12}\,]$

	U^{11}	U^{22}	U^{33}	U^{23}	U^{13}	U^{12}
P(1)	19(1)	17(1)	14(1)	1(1)	3(1)	8(1)
N(2)	18(1)	16(1)	14(1)	-1(1)	2(1)	6(1)
N(3)	21(1)	18(1)	14(1)	-1(1)	4(1)	8(1)
N(4)	18(1)	19(1)	19(1)	1(1)	4(1)	8(1)
C(5)	26(1)	23(1)	17(1)	-4(1)	3(1)	10(1)
C(6)	20(1)	24(1)	25(1)	4(1)	7(1)	10(1)
C(11)	17(1)	15(1)	14(1)	1(1)	1(1)	9(1)
C(12)	22(1)	17(1)	14(1)	1(1)	3(1)	9(1)
C(13)	25(1)	18(1)	19(1)	2(1)	7(1)	8(1)
C(14)	25(1)	16(1)	22(1)	0(1)	5(1)	7(1)
C(15)	24(1)	16(1)	18(1)	-1(1)	2(1)	8(1)
C(16)	19(1)	16(1)	14(1)	1(1)	2(1)	10(1)
C(21)	18(1)	15(1)	16(1)	0(1)	-1(1)	9(1)
C(22)	22(1)	19(1)	17(1)	-2(1)	0(1)	10(1)
C(23)	26(1)	21(1)	20(1)	-4(1)	-3(1)	11(1)
C(24)	23(1)	19(1)	25(1)	-3(1)	-6(1)	9(1)
C(25)	18(1)	18(1)	25(1)	0(1)	-2(1)	8(1)
C(26)	18(1)	17(1)	18(1)	1(1)	1(1)	10(1)

Table S12. Hydrogen coordinates (x 10^4) and isotropic displacement parameters (Å^2x 10^3) for **1**•[H]$_2$.

	x	y	z	U(eq)
H(1A)	3854(6)	1757(6)	10220(19)	20
H(1B)	4286(6)	1456(6)	9496(19)	20
H(5A)	4891	2747	11176	34
H(5B)	4273	2488	11261	34
H(5C)	4610	3006	10131	34
H(6A)	2731	983	8206	35
H(6B)	3058	1252	9959	35
H(6C)	2955	692	9378	35
H(12)	5018	2157	3721	22
H(13)	5759	2989	3673	26
H(14)	5961	3550	6066	27
H(15)	5415	3297	8570	24
H(22)	4414	1427	3200	24
H(23)	3733	707	1760	27
H(24)	2927	228	3101	28
H(25)	2775	460	5930	25

Table S13. Torsion angles [°] for **1**•[H]$_2$.

_____

N(3)-P(1)-N(2)-C(11)	9.03(8)
N(4)-P(1)-N(2)-C(11)	155.85(8)
N(3)-P(1)-N(2)-C(21)	-160.83(8)
N(4)-P(1)-N(2)-C(21)	-14.01(7)
N(4)-P(1)-N(3)-C(16)	-87.50(10)
N(2)-P(1)-N(3)-C(16)	-9.98(8)
N(4)-P(1)-N(3)-C(5)	99.16(11)
N(2)-P(1)-N(3)-C(5)	176.68(9)
N(3)-P(1)-N(4)-C(26)	91.91(10)
N(2)-P(1)-N(4)-C(26)	14.34(8)
N(3)-P(1)-N(4)-C(6)	-98.95(11)
N(2)-P(1)-N(4)-C(6)	-176.53(9)
C(21)-N(2)-C(11)-C(12)	-18.70(18)
P(1)-N(2)-C(11)-C(12)	173.29(9)
C(21)-N(2)-C(11)-C(16)	162.05(10)
P(1)-N(2)-C(11)-C(16)	-5.96(10)
N(2)-C(11)-C(12)-C(13)	-178.22(10)
C(16)-C(11)-C(12)-C(13)	0.97(15)
C(11)-C(12)-C(13)-C(14)	0.15(17)
C(12)-C(13)-C(14)-C(15)	-0.70(18)
C(13)-C(14)-C(15)-C(16)	0.10(17)
C(14)-C(15)-C(16)-N(3)	-179.79(10)
C(14)-C(15)-C(16)-C(11)	1.05(16)
C(5)-N(3)-C(16)-C(15)	3.32(16)
P(1)-N(3)-C(16)-C(15)	-170.35(9)
C(5)-N(3)-C(16)-C(11)	-177.45(9)
P(1)-N(3)-C(16)-C(11)	8.88(11)
C(12)-C(11)-C(16)-C(15)	-1.60(15)
N(2)-C(11)-C(16)-C(15)	177.75(9)
C(12)-C(11)-C(16)-N(3)	179.13(9)
N(2)-C(11)-C(16)-N(3)	-1.53(12)
C(11)-N(2)-C(21)-C(22)	23.11(18)
P(1)-N(2)-C(21)-C(22)	-168.83(9)
C(11)-N(2)-C(21)-C(26)	-157.73(10)

P(1)-N(2)-C(21)-C(26)	10.32(10)
N(2)-C(21)-C(22)-C(23)	179.11(10)
C(26)-C(21)-C(22)-C(23)	0.03(15)
C(21)-C(22)-C(23)-C(24)	-0.01(16)
C(22)-C(23)-C(24)-C(25)	0.22(17)
C(23)-C(24)-C(25)-C(26)	-0.46(16)
C(24)-C(25)-C(26)-N(4)	-179.52(10)
C(24)-C(25)-C(26)-C(21)	0.48(15)
C(6)-N(4)-C(26)-C(25)	-1.21(16)
P(1)-N(4)-C(26)-C(25)	168.29(9)
C(6)-N(4)-C(26)-C(21)	178.79(9)
P(1)-N(4)-C(26)-C(21)	-11.71(11)
N(2)-C(21)-C(26)-C(25)	-179.54(9)
C(22)-C(21)-C(26)-C(25)	-0.28(15)
N(2)-C(21)-C(26)-N(4)	0.47(12)
C(22)-C(21)-C(26)-N(4)	179.73(9)

_____

Symmetry transformations used to generate equivalent atoms:

V. DFT and TDDFT Calculations.

All species were modeled as previously described[20-22] with the B3LYP-D3 flavor of density functional theory as implemented by Gaussian09.[27] This functional combines Becke's three-parameter exchange functional[28] with the correlation functional of Lee, Yang and Parr.[29] Empirical dispersion corrections were added with Grimme's D3 protocol.[30] Nonmetals were modeled with Pople's split-valence double-ζ plus polarization basis set 6-31G(d,p).[31,32] Ru was modeled with the effective core potential of Hay and Wadt[33] and the accompanying uncontracted basis set[34] augmented with f polarization functions[35] collectively known as LANL08(f). All species were modeled in the gas phase. Time-dependent density functional theory (TDDFT) calculations were subsequently performed as described previously[20-22] in order to approximate excitation energies and amplitudes (oscillator strengths) for specific excited states, as well as to simulate the P K-edge XAS data. As previously discussed, [20] an energy shift of +49.6 eV was applied to the calculated spectra to account for the errors in the accuracy of the simulated spectra in including these errors as well as errors associated with relativistic effects and general inaccuracy of the functional. The scalar energy shift was determined by comparing the experimental and calculated energies of the first feature in each spectra. Natural transition orbital analysis was performed on the TDDFT generated transition densities to further validate the assignments of individual excitations in the simulated spectra.[36]
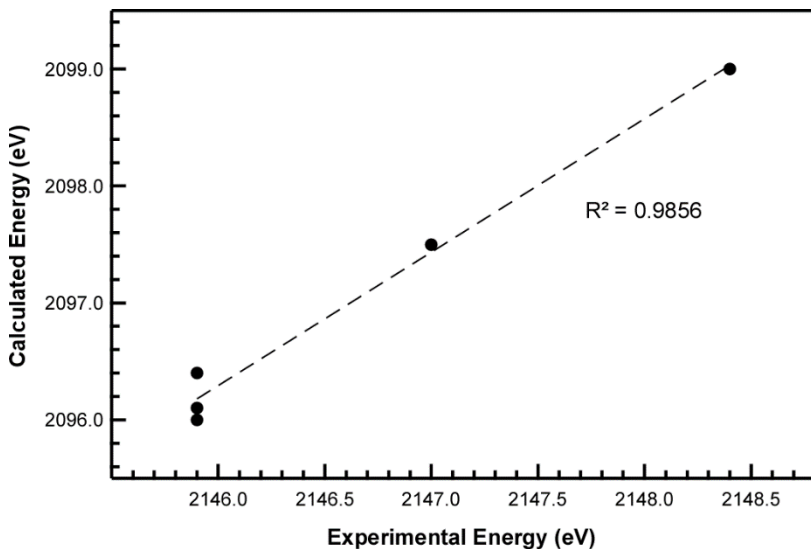

Figure S5. Correlation plot of the unshifted calculated (TDDFT) and experimental energies of the first feature in the P K-edge XAS spectra of P(NMePh)$_3$, 1, 1•[H]$_2$, 2•[Ru], and 2•[H][Ru].

Table S14. Experimental and calculated (TDDFT) P K-edge XANES peak positions (eV). Peak positions were determined by analysis of the 2nd derivative trace of the experimental and simulated spectra.

P(NMePh)$_3$		1		1•[H]$_2$		2•[Ru]		2•[H][Ru]	
Expt	Calc	Expt	Calc	Expt	Calc	Expt	Calc	Expt	Calc
2147.0	2147.1	2145.9	2146.0	2148.4	2148.6	2145.9	2145.6	2145.9	2145.7
2147.4		2147.5	2147.7	2149.7	2149.5		2145.8		2146.1
2148.6	2148.4	2148.4	2148.1	2150.7	2150.5		2146.1	2147.0	2146.6
2149.4	2149.5	2148.6	2148.9		2150.8	2146.8	2146.9		2147.0
	2151.0	2149.6	2149.6		2151.3		2147.5		2147.2
			2150.6			2148.1	2147.9	2147.5	2148.0
							2148.2	2148.2	2148.3
						2149.0	2148.7		2149.1
						2149.7	2149.4	2149.5	2149.4

Table S15. Calculated P 3p orbital composition and energy of selected MOs in P(NMePh)$_3$, C_{2v}-**1**, **1**, and **1**•[H]$_2$. The dashed line indicates the break between occupied and unoccupied MOs (HOMO/LUMO gap).

P(NMePh)$_3$			C_{2v}-1			1			1•[H]$_2$			
MO	E (eV)	P 3p	MO	E (eV)	P 3p	MO	E (eV)	P 3p	MO	E (eV)	P 3p	H 1s
104	2.70	2.6%	78	3.71	20.3%	78	3.41	30.2%	79	3.39	2.0%	0.3%
103	2.58	10.7%	77	3.16	4.9%	77	3.25	1.2%	78	3.29	19.5%	21.4%
102	2.02	2.2%	76	3.05	12.3%	76	2.85	2.6%	77	2.97	20.9%	-
101	1.49	53.2%	75	2.74	6.8%	75	2.75	4.2%	76	2.65	2.5%	7.4%
100	1.40	47.4%	74	2.56	6.3%	74	2.35	3.6%	75	2.51	45.6%	-
99	0.49	2.3%	73	1.63	56.2%	73	1.91	64.1%	74	2.24	11.4%	15.3%
98	0.29	7.7%	72	0.92	2.6%	72	0.55	7.7%	73	1.41	27.5%	5.6%
97	0.19	1.4%	71	0.63	4.4%	71	0.44	8.8%	72	1.04	1.4%	0.4%
96	0.13	2.2%	70	0.58	-	70	0.38	5.9%	71	0.65	2.9%	-
95	0.03	7.7%	69	-0.19	0.2%	69	0.14	4.1%	70	0.23	9.9%	1.8%
94	-0.06	5.6%	68	-1.70	43.8%	68	-0.39	56.5%	69	0.07	1.2%	-
93	-5.07	4.6%	67	-5.14	0.4%	67	-4.97	6.1%	68	-4.73	1.4%	5.0%
92	-5.58	1.7%	66	-5.77	23.7%	66	-5.35	1.5%	67	-5.46	1.0%	-
91	-5.83	2.0%	65	-5.89	18.6%	65	-6.16	0.5%	66	-5.94	0.6%	1.5%
90	-6.53	6.3%	64	-6.13	10.4%	64	-6.57	0.1%	65	-6.60	-	-
89	-6.62	0.5%	63	-6.90	0.1%	63	-7.22	25.3%	64	-7.72	1.4%	17.6%
88	-6.72	2.1%							43	-12.86	9.0%	5.6%
87	-6.96	18.4%							42	-13.17	20.9%	11.4%
P 1s	-2098.88		P 1s	-2098.40		P 1s	-2099.00		P 1s	-2100.21		

Table S16. Calculated P and Ru orbital composition and energy of selected MOs from **2**•[Ru] and **2**•[H][Ru].

|	MO	E (eV)	P 3p (2)	P 3p (PPh₃)	Ru 5s	Ru 5p	Ru 4d	H 1s
2•[Ru]	216	2.29	-	23.0%	10.0%	12.5%	0.9%	-
	215	1.97	22.0%	0.1%	-	24.4%	0.8%	-
	212	1.56	24.3%	3.4%	-	42.0%	2.0%	-
	210	0.81	43.3%	0.6%	-	4.2%	11.2%	-
	201	-0.46	3.3%	0.7%	-	0.9%	9.8%	-
	199	-0.57	2.2%	2.7%	0.1%	0.5%	8.9%	-
	198	-0.64	1.3%	2.0%	0.1%	0.2%	8.5%	-
	197	-0.71	4.3%	3.9%	0.6%	1.4%	15.5%	-
	196	-0.90	1.9%	0.5%	0.1%	0.2%	2.2%	-
	195	-0.90	2.4%	0.6%	-	0.8%	1.7%	-
LUMO	194	-1.36	1.9%	-	-	0.8%	4.6%	-
HOMO	193	-5.05	0.6%	-	0.1%	1.0%	46.8%	-
	192	-5.13	0.6%	0.1%	-	0.4%	47.8%	-
	191	-5.53	0.5%	0.1%	0.1%	2.2%	29.0%	-
	151	-10.54	9.7%	-	1.1%	0.4%	5.4%	-
P 1s (PPh₃)		-2097.92						
P 1s (2)		-2099.87						
2•[H][Ru]	224	3.33	4.7%	4.3%	21.1%	10.4%	0.4%	7.5%
	207	0.51	1.6%	0.1%	2.1%	13.2%	8.8%	4.1%
	204	0.27	0.4%	2.1%	2.0%	7.2%	17.3%	0.1%
	202	-0.09	1.6%	3.5%	2.4%	1.1%	10.8%	0.2%
	201	-0.22	2.5%	1.0%	2.4%	1.1%	8.8%	0.7%
	200	-0.28	0.4%	0.7%	0.5%	0.7%	1.6%	0.1%
	199	-0.42	1.7%	2.4%	0.4%	0.3%	7.4%	0.3%
	198	-0.48	2.4%	1.4%	0.2%	-	6.3%	-
	197	-0.60	0.3%	2.1%	0.2%	0.9%	9.2%	0.5%
	196	-0.71	2.8%	2.3%	-	0.5%	4.4%	0.1%
	195	-0.80	0.2%	7.2%	0.1%	-	1.3%	-
	194	-1.01	0.7%	0.4%	0.2%	2.0%	1.6%	1.2%
LUMO	193	-1.22	0.4%	1.6%	0.1%	1.0%	5.0%	0.1%
HOMO	192	-4.62	0.2%	0.1%	0.4%	1.6%	4.6%	3.0%
	191	-5.27	0.1%	-	0.1%	0.1%	18.2%	0.1%
	190	-5.66	0.2%	0.3%	0.3%	1.9%	33.8%	0.7%
	189	-5.83	-	-	0.1%	1.6%	25.7%	0.2%
	188	-5.92	-	0.3%	0.1%	0.3%	6.0%	0.1%
	187	-6.25	1.9%	2.4%	0.3%	2.1%	43.2%	0.8%
	155	-10.01	8.3%	0.1%	0.8%	0.4%	3.4%	2.6%
	120	-13.29	14.1%	0.1%	-	-	0.9%	8.7%
P 1s (PPh₃)		-2098.19						
P 1s (2)		-2099.41						

MO 94

MO 95
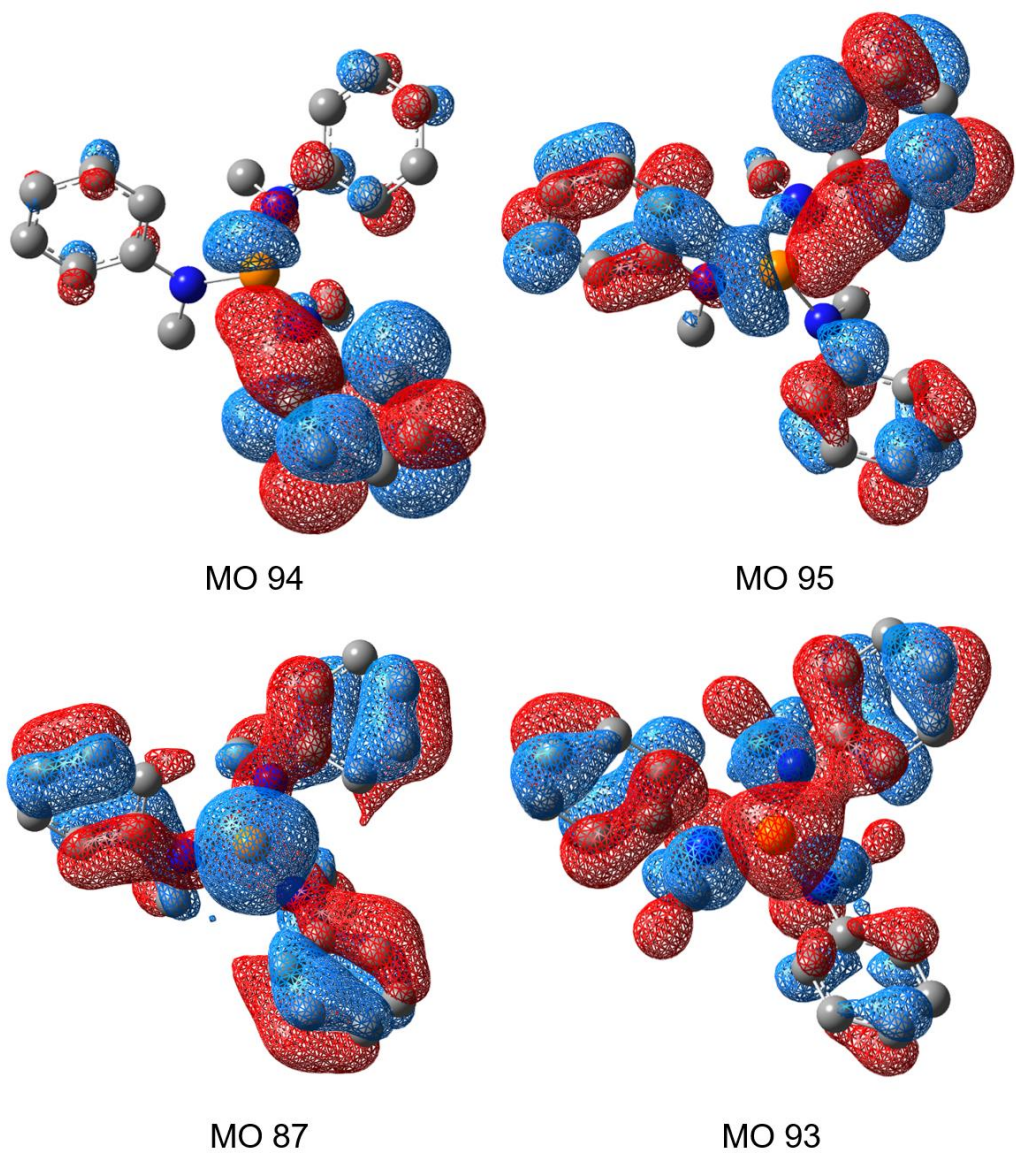
MO 87

MO 93

Figure S6. Kohn-Sham orbitals for MOs 87, 93 (HOMO), 94 (LUMO), and 95 from DFT calculations of $P(NMePh)_3$. Hydrogen atoms are not shown. Despite their similar appearance, MO 93 has significantly less calculated P 3p character than MO 87 (4.6% vs. 18.4%). MO 93 also has less P 3s character than MO 87 (4.4% vs. 10.7%).
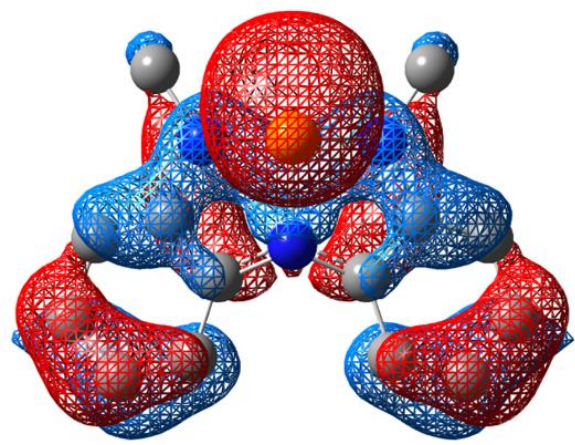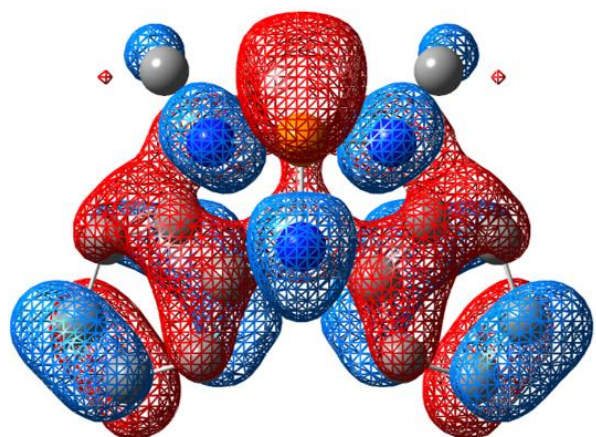
MO 63   MO 67

Figure S7. Kohn-Sham orbitals for MO 63 and MO 67 (HOMO) from DFT calculations of **1**. Hydrogen atoms are not shown.
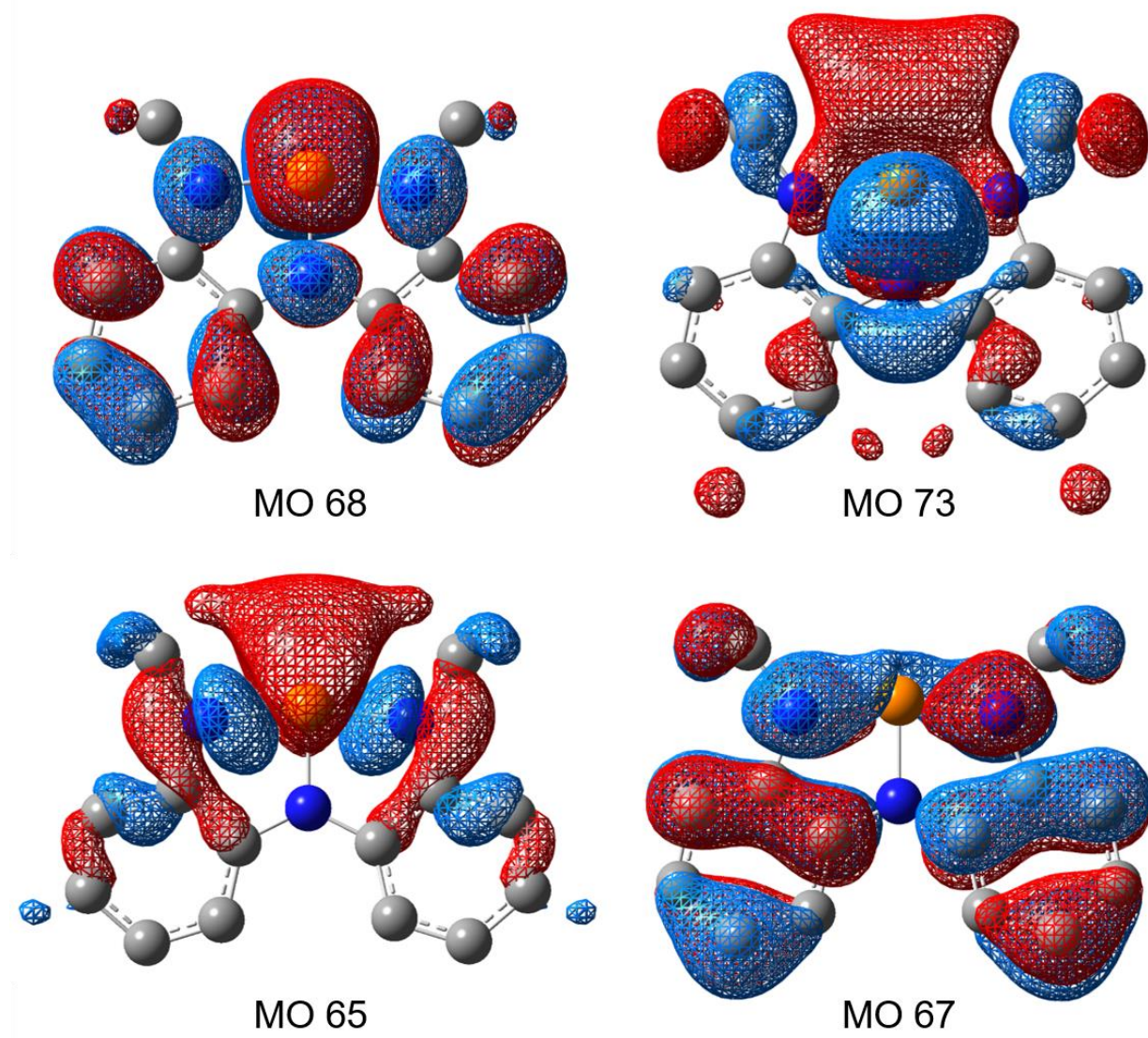
Figure S8. Kohn-Sham orbitals for MOs 65, 67 (HOMO), 68 (LUMO), and 73 from DFT calculations of C_{2v}-**1**. Hydrogen atoms are not shown.

MO 73   MO 74   MO 75

MO 42   MO 43   MO 70
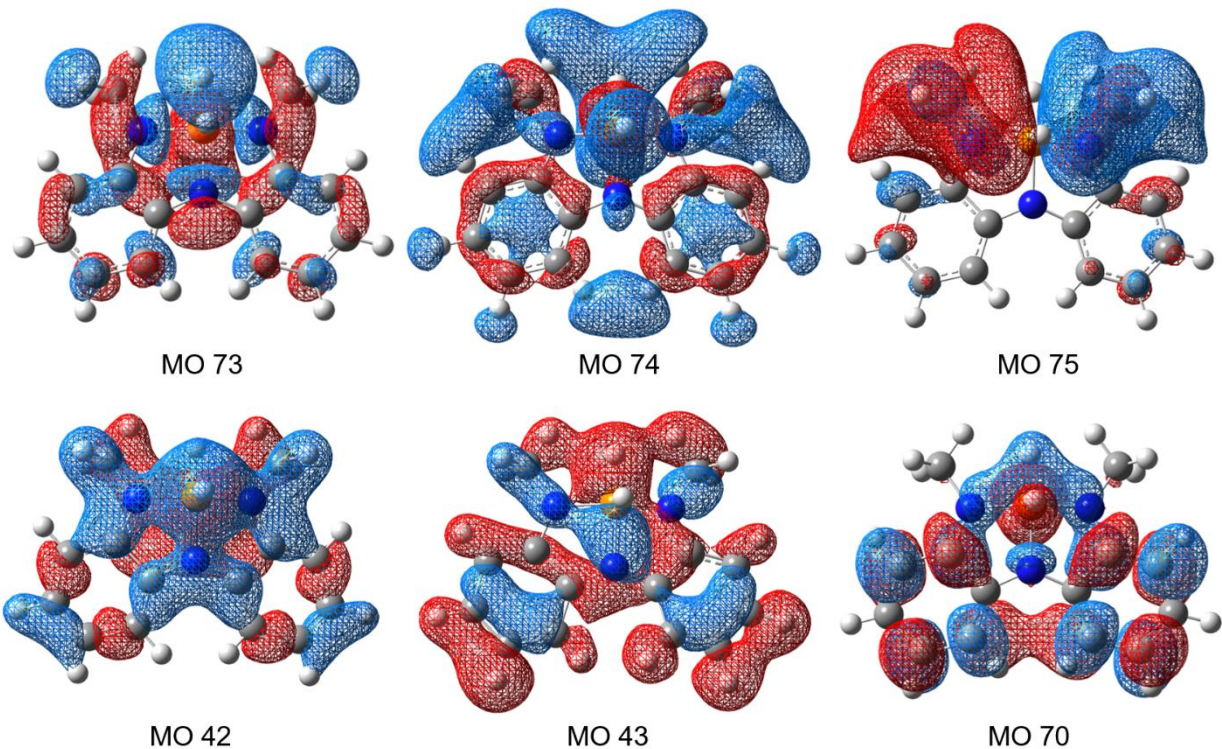
Figure S9. Kohn-Sham orbitals for MOs 42, 43, 70, 73, 74, and 75 from DFT calculations of **1**•[H]$_2$.

MO 212

MO 215

MO 216
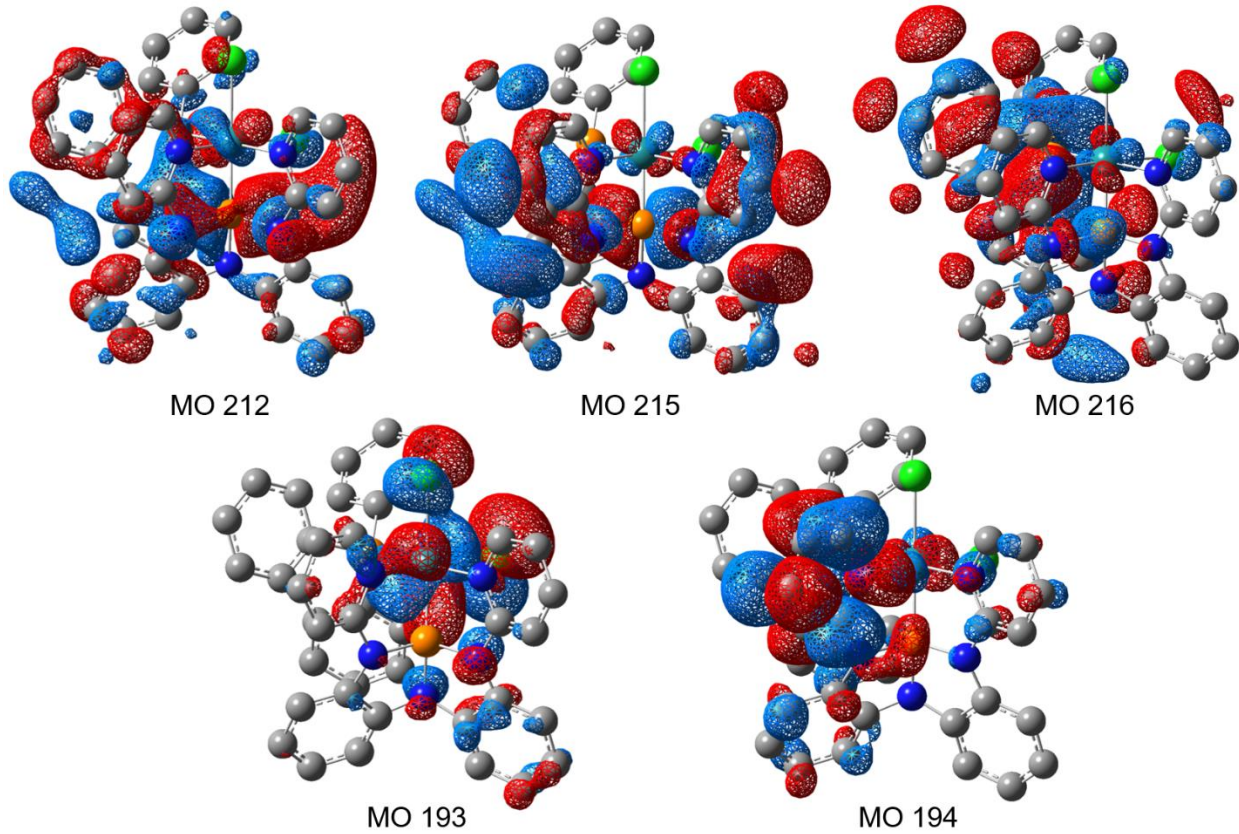
MO 193

MO 194

Figure S10. Kohn-Sham orbitals for MOs 193 (HOMO), 194 (LUMO), 212, 215, and 216 from DFT calculations of **2**•[Ru]. Hydrogen atoms are not shown.

MO 192

MO 193

MO 120
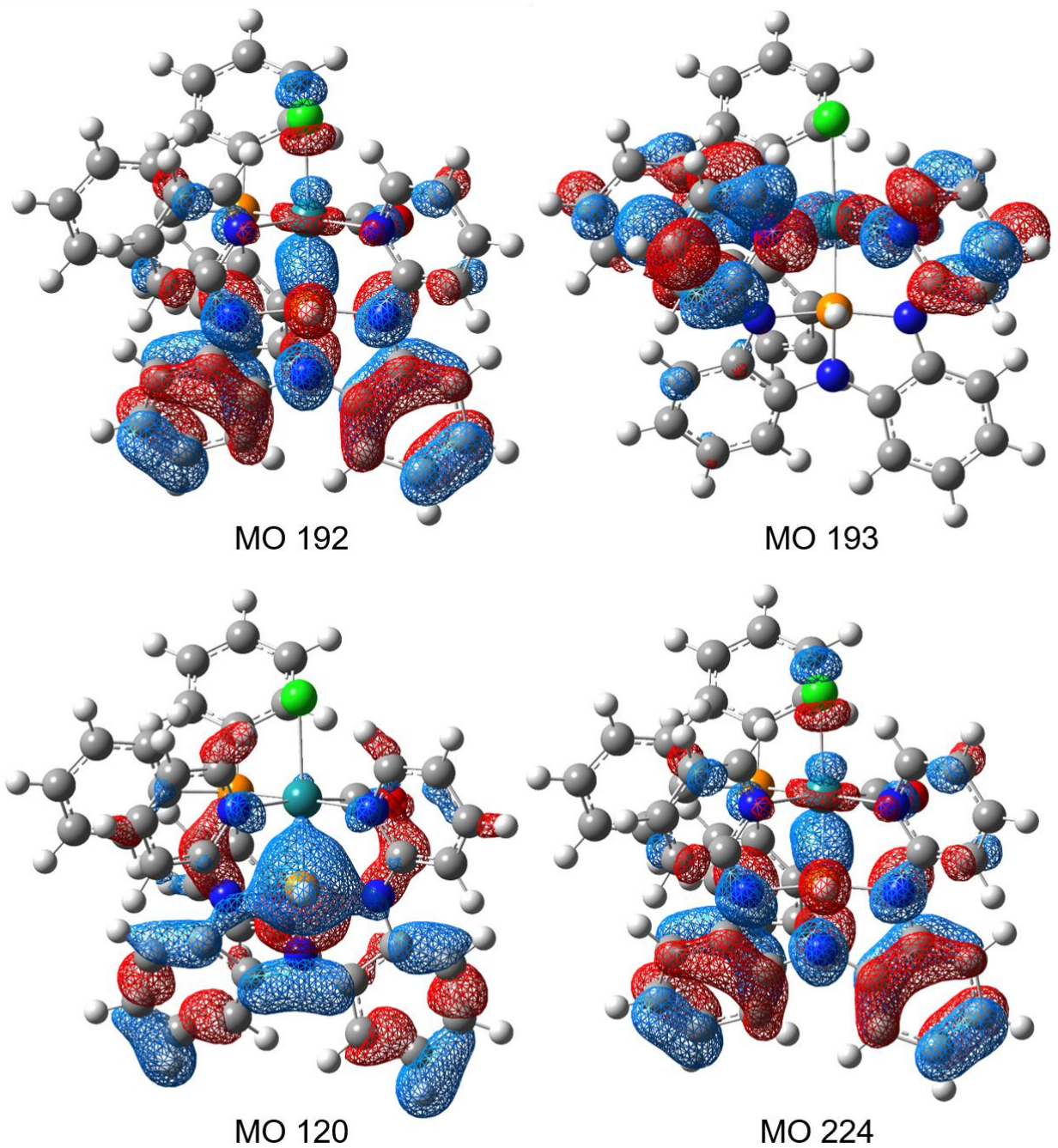
MO 224

Figure S11. Kohn-Sham orbitals for MOs 120, 192 (HOMO), 193 (LUMO), 224 from DFT calculations of **2**•[H][Ru].
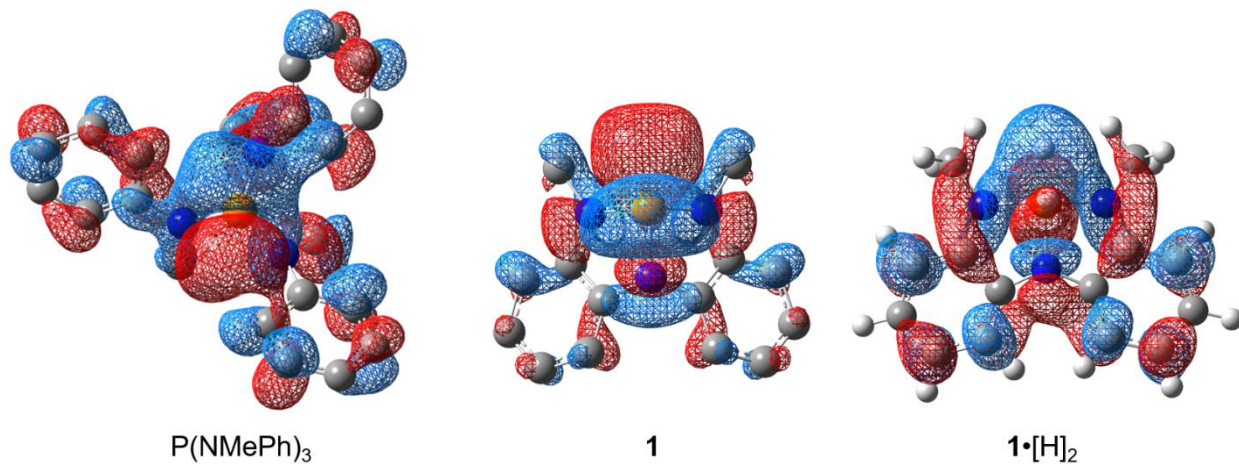
P(NMePh)₃   **1**   **1**•[H]₂

Figure S12. Plot of first natural transition orbitals calculated for P(NMePh)$_3$, **1**, and **1**•[H]$_2$. Hydrogen atoms are not shown on P(NMePh)$_3$ and **1**.
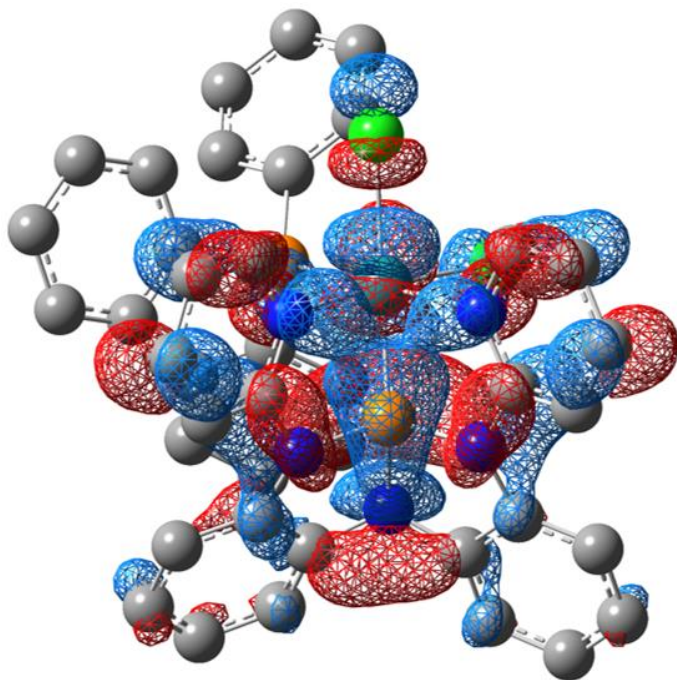

Figure S13. Plot of 14th natural transition orbital corresponding to the intense transition at 2146.8 eV in the P K-edge XAS spectrum of **2**•[Ru] (Figure 3b). Hydrogen atoms are not shown. Calculated composition (most relevant atoms and orbitals): Ru 4d = 16.3%, P 3p (**2**) = 32.8%, P 3p (PPh$_3$) = 0.6%, N 2p = 3.5%.

The calculation of the energies of $P(NH_2)_3$ within C_s symmetry was performed at the B3LYP/6-31G* level of theory. By parameterizing $P(NH_2)_3$ as depicted in Figure 5, 4141 discrete input structures in the range $80° \leq \theta \leq 120°$ and $80° \leq \varphi \leq 180°$ at 1° increments were generated and submitted to optimization within the geometry constraints. The 2D contour maps depicting the energies (Figure 5 and Figure S14) were plotted in Origin 2019 with smoothing to improve clarity.

Within the parameterization, the dihedral angles $\angle$HNPH are not restrained and are free to optimization at each input structure. Consequently, small conformational changes associated with bond rotation about the P–N bonds contributes a small underlying 'waviness' to the energy plots. This effect is most pronounced in the plot of HOMO (Figure S14b), which shows a line of discontinuity at θ=101° arising from a change in preferred conformation in the optimized geometry (Figure S15).
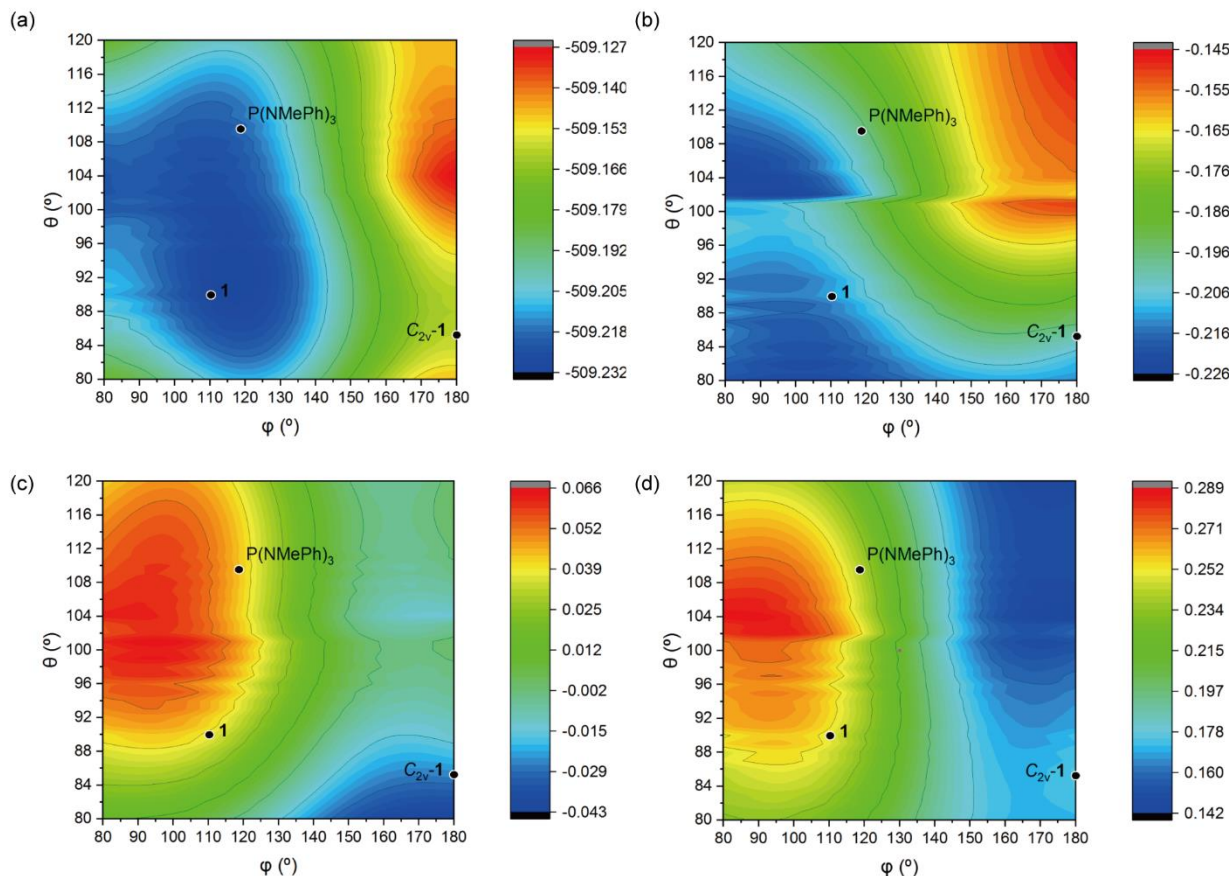
Figure S14. Contour maps depicting the orbital of (a) Total electronic energy, (b) HOMO energies, (c) LUMO energies, (d) ΔHOMO–LUMO for all $P(NH_2)_3$ structures with C_s-symmetry. Energies are shown in a units of Hartrees. Points corresponding to the structures of $P(NMePh)_3$, **1** and C_{2v}-**1** are superimposed as black points.
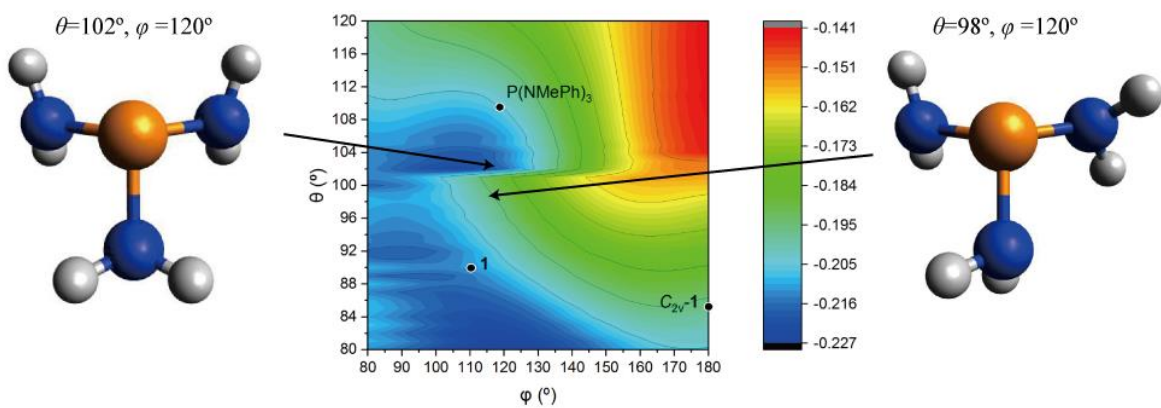
Figure S15. Difference in the conformation of P(NH$_2$)$_3$ between $\theta = 102°$, $\varphi = 120°$ and $\theta = 98°$, $\varphi = 120°$.

Table S17. DFT calculated bond distances (Å) and angles (deg) for P(NMePh)₃, **1**, and C_{2v}-**1**.

	P(NMePh)₃	**1**	**C_{2v}-1**
N_a-P (Å)	1.75463	1.75079	1.85316
N_b-P (Å)	1.75867	1.75085	1.85316
N_c-P (Å)	1.74529	1.78508	1.79691
N_a-P-N_c	101.1644	89.0050	83.1372
N_c-P-N_b	100.7412	89.0041	83.1372
N_a-P-N_b	99.7450	118.3600	166.2743

Table S18. Calculated bond distances (Å) and angles (deg) for **1**•[H₂]**, 2**•[Ru]**,** and **2**•[H][Ru].

	1•[H₂]	**2•[Ru]**	**2•[H][Ru]**
N_a-P (Å)	1.73743	1.76363	1.86703
N_b-P (Å)	1.73927	1.7434	1.87203
N_c-P (Å)	1.81174	1.73199	1.74552
H_a-P (Å)	1.43546	-	1.41729
H_b-P (Å)	1.42045	-	-
Ru-P_a (Å)	-	2.14518	2.28148
Ru-P_b (Å)	-	2.35122	2.37341
Ru-N_d (Å)	-	2.17847	2.27735
Ru-N_e (Å)	-	2.21536	2.23774
Ru-Cl_a (Å)	-	2.50583	2.50792
Ru-Cl_b (Å)	-	2.44612	-
Ru-CO (Å)	-	-	1.85471
N_a-P-N_c	86.4440	90.3278	86.0845
N_c-P-N_b	86.4344	91.1381	86.5703
N_c-P-H_b	97.9698	-	-
N_c-P-H_a	165.0996	-	110.9246
N_a-P-N_b	145.3872	114.2708	169.3796
N_a-P-H_b	107.4010	-	-
N_a-P-H_a	89.2169	-	87.6441
N_b-P-H_b	107.1213	-	-
N_b-P-H_a	89.0884	-	87.9057
H_a-P-H_b	96.9302	-	-
Ru-P-N_a	-	104.5351	96.1406

Ru-P-N$_b$	-	106.2463	141.1131
Ru-P-N$_c$	-	149.3345	94.4039
Ru-P-H$_a$	-	-	107.9580
Cl$_a$-Ru-Cl$_b$	-	92.8719	-
Cl$_b$-Ru-N$_e$	-	84.4527	-
Cl$_b$-Ru-N$_d$	-	174.1291	-
Cl$_b$-Ru-P$_a$	-	94.9372	-
Cl$_b$-Ru-P$_b$	-	93.1039	-
Cl$_a$-Ru-N$_e$	-	92.0802	92.7772
Cl$_a$-Ru-N$_d$	-	90.4287	89.6851
Cl$_a$-Ru-P$_a$	-	167.7370	158.1199
Cl$_a$-Ru-P$_b$	-	89.8473	90.6778
N$_d$-Ru-N$_e$	-	90.5800	97.2803
N$_e$-Ru-P$_a$	-	79.3039	75.1313
N$_e$-Ru-P$_b$	-	176.9588	172.5257
N$_d$-Ru-P$_a$	-	81.0319	74.2068
N$_d$-Ru-P$_b$	-	91.7580	89.3601
P$_a$-Ru-P$_b$	-	99.1413	103.5842
Cl$_a$-Ru-CO	-	-	97.8470
CO-Ru-N$_e$	-	-	83.6315
CO-Ru-N$_d$	-	-	172.3700
CO-Ru-P$_a$	-	-	98.8113
CO-Ru-P$_b$	-	-	89.3342

Table S19. Atomic coordinates and Mulliken charges from DFT calculations of P(NMePh)$_3$, **1**, C_{2v}-**1**, **1**•[H]$_2$, **2**•[Ru], and **2**•[H][Ru].

P(NMePh)$_3$		Coordinates (Å)			Mulliken
Atom #	Atom	x	y	z	Charges
1	P	0.032281	-0.25009	-0.06582	0.8409232
2	N	-1.32768	-0.7966	0.881739	-0.6510361
3	N	1.322871	-1.25562	0.579318	-0.6434773
4	N	0.404592	1.263792	0.739333	-0.6484934
5	C	-1.62271	-0.19594	2.185139	-0.1640698
6	H	-0.70886	-0.12012	2.776816	0.1098363
7	H	-2.05175	0.810868	2.100562	0.121858
8	H	-2.32246	-0.83781	2.72805	0.1179726

Atom #	Atom	x	y	z	Mulliken Charges
9	C	1.40246	1.403935	1.797532	-0.1631009
10	H	1.055555	2.127906	2.543033	0.113534
11	H	1.556463	0.44354	2.288189	0.1192496
12	H	2.376753	1.730275	1.411193	0.1180646
13	C	1.101203	-2.30497	1.568819	-0.1755166
14	H	1.783287	-2.19221	2.422123	0.1077186
15	H	0.074182	-2.25553	1.923641	0.1338906
16	H	1.25332	-3.30287	1.138021	0.1149788
17	C	-2.37965	-1.43284	0.179097	0.2753412
18	C	-2.0779	-2.41643	-0.78059	-0.1182996
19	C	-3.72777	-1.10596	0.407689	-0.1162406
20	C	-3.09467	-3.03448	-1.50478	-0.0979325
21	H	-1.04362	-2.70517	-0.94226	0.1009264
22	C	-4.73958	-1.7499	-0.30537	-0.0988036
23	H	-3.98801	-0.33985	1.129898	0.0844582
24	C	-4.43304	-2.71151	-1.269	-0.0852757
25	H	-2.83774	-3.78866	-2.24327	0.0870788
26	H	-5.77526	-1.48433	-0.11168	0.0843899
27	H	-5.22432	-3.20532	-1.82452	0.0813306
28	C	-0.15698	2.436202	0.192709	0.2836575
29	C	0.50297	3.677089	0.277627	-0.1164173
30	C	-1.41313	2.390729	-0.44796	-0.1340484
31	C	-0.06985	4.823032	-0.2728	-0.0985046
32	H	1.470027	3.748167	0.76206	0.0812623
33	C	-1.96284	3.539293	-1.01334	-0.1009077
34	H	-1.971	1.460436	-0.48829	0.1050391
35	C	-1.30029	4.765316	-0.92892	-0.0870764
36	H	0.460489	5.768264	-0.19361	0.0818987
37	H	-2.92936	3.474274	-1.5054	0.0852256
38	H	-1.73874	5.66049	-1.35897	0.0784234
39	C	2.592102	-1.17381	-0.02785	0.2987649
40	C	3.581029	-2.15297	0.199023	-0.1256714
41	C	2.923658	-0.09142	-0.87422	-0.1448631
42	C	4.831514	-2.05978	-0.41211	-0.0982274
43	H	3.384305	-2.99518	0.850198	0.0777583
44	C	4.171563	-0.02009	-1.48707	-0.1015111
45	H	2.211885	0.707991	-1.04764	0.1124315
46	C	5.140077	-1.00066	-1.26449	-0.0883223
47	H	5.569645	-2.83265	-0.21467	0.0803675
48	H	4.388755	0.823818	-2.13616	0.0843302
49	H	6.114821	-0.93496	-1.73753	0.0770851

1		Coordinates (Å)			Mulliken
Atom #	Atom	x	y	z	Charges

1	C	-2.04681	0.232158	-0.17352	0.30956
2	C	-1.2317	-0.75609	0.419152	0.21685
3	C	1.231603	-0.75618	0.419121	0.216884
4	C	2.046843	0.23202	-0.17345	0.309535
5	P	5.53E-05	1.56155	0.858179	0.701031
6	N	-6.5E-06	-0.22304	0.900206	-0.68238
7	N	-1.50349	1.510072	-0.03747	-0.6059
8	N	1.503651	1.51	-0.03725	-0.60588
9	C	-2.28652	2.704384	-0.29221	-0.16631
10	H	-3.28066	2.629515	0.16612	0.119304
11	H	-1.76983	3.56628	0.142223	0.114566
12	H	-2.41345	2.891367	-1.3661	0.119407
13	C	2.286861	2.704234	-0.29188	-0.16631
14	H	1.770213	3.56619	0.142477	0.114572
15	H	3.280935	2.629229	0.166564	0.119311
16	H	2.413935	2.891194	-1.36576	0.11941
17	C	1.661016	-2.07618	0.471944	-0.10931
18	C	3.269731	-0.10997	-0.74888	-0.13383
19	C	-1.66123	-2.07605	0.472096	-0.10931
20	C	-3.26973	-0.10979	-0.74892	-0.13384
21	H	1.059742	-2.83301	0.960265	0.086235
22	H	3.889626	0.646427	-1.21896	0.081466
23	H	-1.06	-2.83287	0.960479	0.086238
24	H	-3.88956	0.646602	-1.21909	0.081464
25	C	2.893592	-2.41944	-0.1031	-0.10665
26	C	3.686743	-1.44687	-0.70706	-0.09461
27	C	-2.89387	-2.41924	-0.10289	-0.10666
28	C	-3.68691	-1.44664	-0.70691	-0.0946
29	H	-4.64307	-1.71945	-1.14374	0.079913
30	H	-3.22932	-3.451	-0.06615	0.079968
31	H	3.228919	-3.45125	-0.06648	0.079969
32	H	4.64286	-1.71976	-1.14392	0.079915

C_{2v}-**1**			**Coordinates (Å)**		**Mulliken**
Atom #	**Atom**	**x**	**y**	**z**	**Charges**
1	C	-2.30954	0.233616	0.084769	0.28514
2	C	-1.24842	-0.70403	-0.0405	0.27446
3	C	1.248418	-0.70403	0.040535	0.274459
4	C	2.30954	0.23362	-0.08478	0.28514
5	P	-1.8E-06	1.723467	2.73E-05	0.579799
6	N	-2E-07	-0.07345	2.57E-05	-0.70537
7	N	-1.83385	1.502026	0.148828	-0.59457
8	N	1.833848	1.50203	-0.14882	-0.59457
9	C	-2.69572	2.660314	0.22501	-0.17086

10	H	-3.27694	2.673981	1.155924	0.115631
11	H	-2.06553	3.555938	0.201044	0.118885
12	H	-3.39573	2.706212	-0.61935	0.113793
13	C	2.695709	2.660319	-0.22503	-0.17086
14	H	2.06552	3.555943	-0.20101	0.118884
15	H	3.395765	2.706202	0.619289	0.113792
16	H	3.276875	2.674002	-1.15598	0.115631
17	C	1.555412	-2.05596	0.264543	-0.10679
18	C	3.650259	-0.19799	-0.08646	-0.11701
19	C	-1.5554	-2.05597	-0.2645	-0.10679
20	C	-3.65026	-0.198	0.086396	-0.11701
21	H	0.784839	-2.77994	0.480465	0.096627
22	H	4.45051	0.525413	-0.20162	0.085228
23	H	-0.78482	-2.77995	-0.48039	0.096625
24	H	-4.45052	0.52541	0.201524	0.085228
25	C	2.885319	-2.46619	0.275098	-0.10844
26	C	3.927653	-1.54682	0.080001	-0.09596
27	C	-2.88531	-2.4662	-0.2751	-0.10844
28	C	-3.92765	-1.54682	-0.08005	-0.09596
29	H	-4.95825	-1.88958	-0.08278	0.083836
30	H	-3.11297	-3.51276	-0.45198	0.082818
31	H	3.112989	-3.51275	0.451989	0.082818
32	H	4.958254	-1.88957	0.0827	0.083836

1•[H]$_2$			Coordinates (Å)		Mulliken
Atom #	Atom	x	y	z	Charges
1	C	2.230491	0.195315	0.019991	0.273275
2	C	1.257696	-0.81886	-0.15878	0.286462
3	C	-1.26874	-0.80583	-0.18327	0.283423
4	C	-2.21968	0.214131	0.068326	0.274004
5	P	0.001798	1.55217	-0.50003	0.916195
6	N	-0.00032	-0.25477	-0.36827	-0.75767
7	N	1.674759	1.475899	-0.03737	-0.59348
8	N	-1.64306	1.486578	0.061414	-0.59472
9	C	2.492769	2.637995	0.248883	-0.17188
10	H	3.249884	2.804163	-0.52856	0.119759
11	H	1.860018	3.527514	0.299078	0.116652
12	H	3.005717	2.523645	1.211836	0.121541
13	C	-2.44163	2.652001	0.385052	-0.17193
14	H	-1.79631	3.53172	0.446144	0.116772
15	H	-3.21032	2.846298	-0.37482	0.118479
16	H	-2.93937	2.521772	1.353795	0.121805
17	C	-1.68365	-2.13644	-0.21684	-0.11734
18	C	-3.55608	-0.09675	0.299575	-0.13448

19	C	1.643108	-2.1569	-0.083	-0.11405
20	C	3.563962	-0.12536	0.253839	-0.13464
21	H	-0.98935	-2.93294	-0.44524	0.087192
22	H	-4.27941	0.68883	0.490262	0.077255
23	H	0.924543	-2.95466	-0.20647	0.082266
24	H	4.304063	0.65698	0.383412	0.077005
25	C	-3.03222	-2.44424	0.014288	-0.10418
26	C	-3.95907	-1.43922	0.272837	-0.10108
27	C	2.988645	-2.47484	0.151444	-0.10392
28	C	3.941333	-1.47407	0.314533	-0.10162
29	H	4.982095	-1.7312	0.486344	0.075729
30	H	3.282416	-3.51921	0.197914	0.076596
31	H	-3.34965	-3.48207	-0.02065	0.076952
32	H	-5.00186	-1.68772	0.445256	0.076266
33	H	-0.04331	1.646399	-1.91663	-0.03993
34	H	0.012593	2.962511	-0.23288	-0.1367

| 2•[Ru] | | | Coordinates (Å) | | Mulliken |
Atom #	Atom	x	y	z	Charges
1	Ru	-0.17981	1.315749	-0.21157	-0.20497
2	Cl	0.269319	1.683505	-2.58782	-0.34561
3	Cl	-1.89276	3.142558	-0.12337	-0.44788
4	N	1.48104	2.747568	0.10349	-0.49425
5	C	1.255862	4.062672	0.268121	0.133123
6	C	2.76373	2.296424	0.089216	0.507629
7	C	2.281091	4.985333	0.439475	-0.11573
8	H	0.20924	4.349362	0.247008	0.169534
9	C	3.841957	3.160166	0.318836	-0.12225
10	C	3.593856	4.518517	0.48178	-0.06245
11	H	2.04474	6.037158	0.552211	0.108404
12	H	4.843362	2.764021	0.409082	0.111517
13	H	4.421706	5.19968	0.654534	0.107765
14	N	-0.36152	1.019183	1.938951	-0.48989
15	C	-1.17248	1.768117	2.714003	0.123524
16	C	0.396173	0.059083	2.543743	0.469995
17	C	-1.26643	1.602916	4.089772	-0.10173
18	H	-1.75966	2.502524	2.173671	0.165907
19	C	0.399585	-0.1147	3.93153	-0.11706
20	C	-0.4547	0.655561	4.711529	-0.06806
21	H	-1.95756	2.2191	4.653088	0.107263
22	H	1.083826	-0.82541	4.376498	0.11451
23	H	-0.473	0.524713	5.789159	0.106631
24	P	1.460811	-0.03533	0.079473	1.041831
25	P	-1.88033	-0.2493	-0.64415	0.669877

26	N	2.911934	0.916515	-0.08691	-0.69825
27	N	1.208647	-0.6963	1.695001	-0.6835
28	N	2.308372	-1.47199	-0.38684	-0.69728
29	C	3.957959	0.19318	-0.70898	0.30731
30	C	5.171818	0.658259	-1.21104	-0.12008
31	C	3.612295	-1.17063	-0.86456	0.220468
32	C	6.054601	-0.24789	-1.81116	-0.09567
33	H	5.428806	1.707355	-1.17149	0.097464
34	C	4.492037	-2.06274	-1.46315	-0.1053
35	C	5.730164	-1.59765	-1.92068	-0.10122
36	H	6.998335	0.118741	-2.20258	0.090137
37	H	4.215332	-3.10233	-1.58435	0.088408
38	H	6.42381	-2.29122	-2.38501	0.089437
39	C	1.404232	-2.09755	1.705518	0.288962
40	C	0.996718	-3.02703	2.660423	-0.13852
41	C	2.01132	-2.53932	0.504636	0.222119
42	C	1.215633	-4.38974	2.417353	-0.09255
43	H	0.494109	-2.71144	3.565389	0.092672
44	C	2.198937	-3.89213	0.261758	-0.09873
45	C	1.815361	-4.82104	1.236945	-0.10324
46	H	0.895018	-5.11414	3.159746	0.089611
47	H	2.597649	-4.22181	-0.68884	0.102087
48	H	1.963231	-5.88046	1.054702	0.089601
49	C	-3.20509	0.129074	-1.86642	-0.13534
50	C	-3.16798	1.282566	-2.65798	-0.06003
51	C	-4.26219	-0.78476	-2.01899	-0.07752
52	C	-4.18458	1.515974	-3.58855	-0.0913
53	H	-2.35487	1.987273	-2.54928	0.171093
54	C	-5.27382	-0.54351	-2.94477	-0.09209
55	H	-4.29488	-1.68572	-1.41318	0.087974
56	C	-5.23548	0.611156	-3.7327	-0.08269
57	H	-4.14864	2.413591	-4.19886	0.093391
58	H	-6.0883	-1.25434	-3.0532	0.081187
59	H	-6.02342	0.800363	-4.45676	0.083497
60	C	-1.28817	-1.89654	-1.24341	-0.13684
61	C	-1.82054	-3.12373	-0.81705	-0.09881
62	C	-0.28823	-1.89504	-2.23076	-0.09312
63	C	-1.33427	-4.32443	-1.33581	-0.08185
64	H	-2.61064	-3.15061	-0.07489	0.095642
65	C	0.185676	-3.09781	-2.75417	-0.08769
66	H	0.113106	-0.95167	-2.59051	0.152816
67	C	-0.32683	-4.31504	-2.30198	-0.08695
68	H	-1.74566	-5.26635	-0.98415	0.084226
69	H	0.962577	-3.07812	-3.51317	0.092471
70	H	0.050899	-5.25117	-2.70408	0.082947

71	C	-2.82246	-0.58404	0.901279	-0.12493
72	C	-3.94593	0.202739	1.197846	-0.09729
73	C	-2.33477	-1.46661	1.87821	-0.12348
74	C	-4.57974	0.089179	2.435964	-0.08667
75	H	-4.31379	0.913412	0.465674	0.133094
76	C	-2.97226	-1.57922	3.113406	-0.08414
77	H	-1.45327	-2.0669	1.679407	0.1021
78	C	-4.09839	-0.80322	3.395598	-0.08827
79	H	-5.44919	0.704052	2.650261	0.092487
80	H	-2.58333	-2.27018	3.856286	0.07971
81	H	-4.59379	-0.8901	4.358512	0.08482

| 2•[H][Ru] | | Coordinates (Å) | | | Mulliken |
Atom #	Atom	x	y	z	Charges
1	Ru	0.051723	-1.4126	0.007698	-0.21344
2	Cl	-1.49345	-3.38757	-0.03261	-0.42483
3	N	1.843984	-2.66756	-0.46171	-0.50991
4	C	1.750158	-3.96034	-0.82124	0.121134
5	C	3.077431	-2.12665	-0.18018	0.46806
6	C	2.854649	-4.79259	-0.92734	-0.12116
7	H	0.738057	-4.31345	-0.99029	0.155662
8	C	4.23746	-2.91913	-0.29687	-0.11671
9	C	4.117407	-4.25025	-0.66359	-0.06597
10	H	2.725543	-5.8316	-1.20707	0.101322
11	H	5.207945	-2.46986	-0.13794	0.105573
12	H	5.00993	-4.86238	-0.7579	0.104246
13	N	-0.53179	-0.92814	-2.13966	-0.50588
14	C	-1.15969	-1.80351	-2.94623	0.109183
15	C	-0.33949	0.360641	-2.57392	0.47852
16	C	-1.66782	-1.45419	-4.18806	-0.11919
17	H	-1.28515	-2.79754	-2.53019	0.148237
18	C	-0.84156	0.780002	-3.82092	-0.10622
19	C	-1.51286	-0.13129	-4.61914	-0.06501
20	H	-2.18141	-2.19404	-4.79092	0.097119
21	H	-0.65541	1.791916	-4.15529	0.104326
22	H	-1.89807	0.182206	-5.58521	0.100829
23	P	1.619953	0.064243	-0.74379	0.971526
24	P	-1.70798	-0.01582	0.77289	0.643841
25	N	3.046692	-0.79077	0.116723	-0.71426
26	N	0.443467	1.112477	-1.74523	-0.71829
27	N	2.393689	1.565655	-0.30342	-0.7373
28	C	4.03042	0.083692	0.553999	0.284077
29	C	5.217726	-0.20297	1.229687	-0.12984
30	C	3.668336	1.438475	0.293817	0.262746

31	C	6.090048	0.835799	1.575224	-0.09901
32	H	5.450848	-1.22396	1.505757	0.093703
33	C	4.56924	2.456314	0.602236	-0.12794
34	C	5.779733	2.149192	1.239776	-0.10479
35	H	7.011668	0.606091	2.10098	0.081953
36	H	4.361312	3.479503	0.327321	0.09171
37	H	6.469354	2.953442	1.476421	0.080974
38	C	0.615663	2.474344	-1.57177	0.290501
39	C	-0.17469	3.523536	-2.04366	-0.13407
40	C	1.700463	2.737657	-0.68561	0.264981
41	C	0.086406	4.831474	-1.61806	-0.10195
42	H	-1.01663	3.317194	-2.69174	0.089489
43	C	1.906326	4.036143	-0.22583	-0.1179
44	C	1.106285	5.08257	-0.70604	-0.10303
45	H	-0.53078	5.64511	-1.98713	0.078795
46	H	2.649183	4.242418	0.530385	0.092961
47	H	1.285216	6.091327	-0.34754	0.080002
48	C	-2.94916	-0.81627	1.889573	-0.09381
49	C	-2.55023	-1.81726	2.785836	-0.07092
50	C	-4.28683	-0.38878	1.90505	-0.10027
51	C	-3.463	-2.36425	3.687223	-0.0817
52	H	-1.53712	-2.19414	2.771218	0.115612
53	C	-5.19897	-0.94063	2.804763	-0.0872
54	H	-4.62737	0.36497	1.203183	0.09773
55	C	-4.78846	-1.92819	3.701113	-0.08315
56	H	-3.13668	-3.14388	4.369098	0.09374
57	H	-6.23089	-0.60097	2.798882	0.085105
58	H	-5.49898	-2.36144	4.399374	0.087463
59	C	-1.22043	1.463072	1.773038	-0.10953
60	C	-2.19896	2.352803	2.253099	-0.08299
61	C	0.119093	1.703134	2.100858	-0.08684
62	C	-1.83792	3.46714	3.00627	-0.08609
63	H	-3.24722	2.175699	2.037835	0.097086
64	C	0.481013	2.817544	2.860817	-0.07799
65	H	0.891422	1.024691	1.767859	0.111125
66	C	-0.49392	3.705977	3.308563	-0.08259
67	H	-2.60667	4.147377	3.36155	0.089922
68	H	1.528492	2.98392	3.093548	0.097008
69	H	-0.21382	4.576195	3.895197	0.090403
70	C	-2.78453	0.647	-0.56315	-0.14908
71	C	-3.51969	-0.29154	-1.30789	-0.10266
72	C	-2.87197	2.004593	-0.89038	-0.10908
73	C	-4.3394	0.130073	-2.35156	-0.08134
74	H	-3.43436	-1.34843	-1.06835	0.148715
75	C	-3.69636	2.421749	-1.93904	-0.09112

76	H	-2.29228	2.738507	-0.34366	0.116705
77	C	-4.4321	1.488733	-2.66871	-0.08672
78	H	-4.89944	-0.60375	-2.92355	0.09208
79	H	-3.75692	3.478844	-2.18293	0.087631
80	H	-5.07185	1.815287	-3.48375	0.087165
81	C	0.642947	-1.58931	1.756745	0.330942
82	O	1.048045	-1.69408	2.839525	-0.30326
83	H	2.132167	-0.42854	-1.96996	-0.02688

VI. Multinuclear NMR Spectra
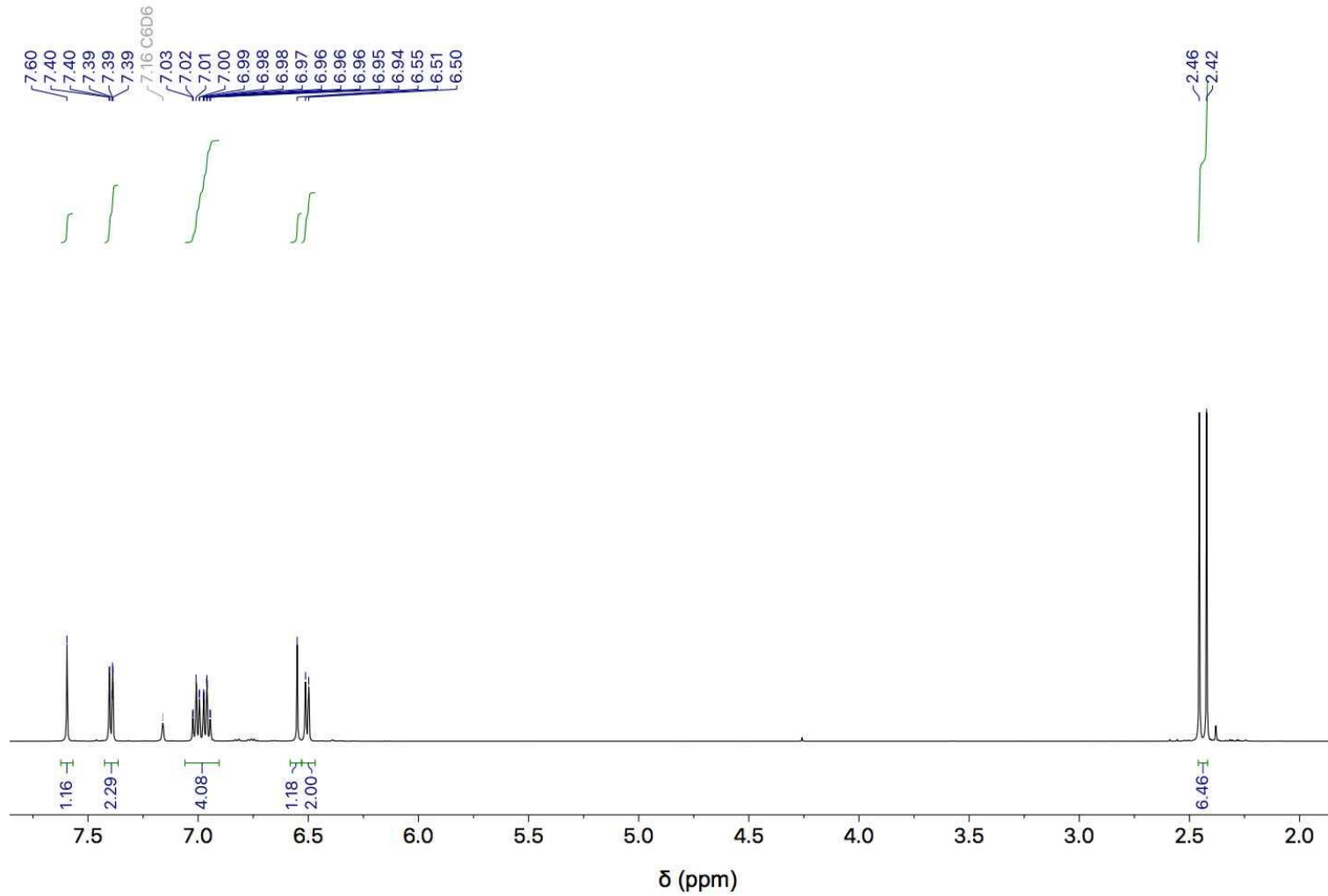
Figure S16. ^{1}H NMR spectrum of **1•[H]₂**
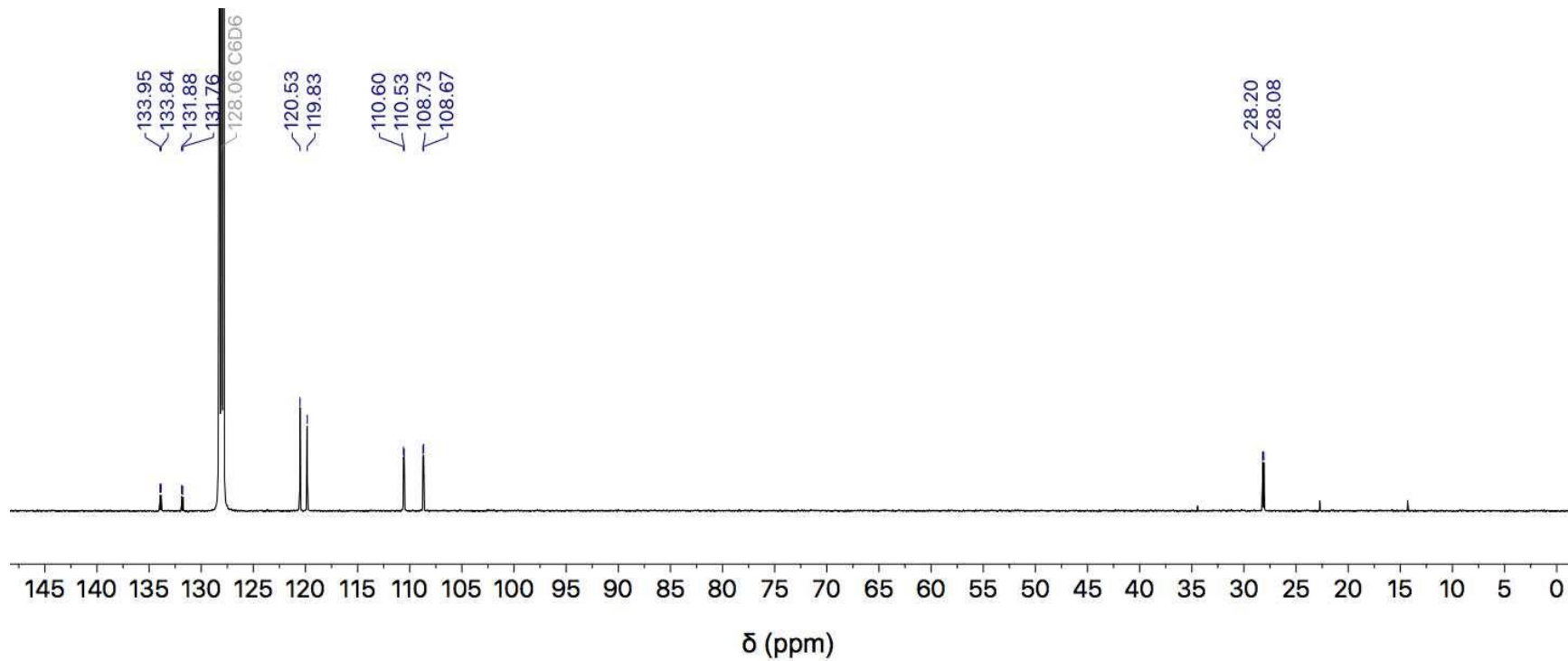
Figure S17. ^{13}C NMR spectrum of **1•[H]₂**.
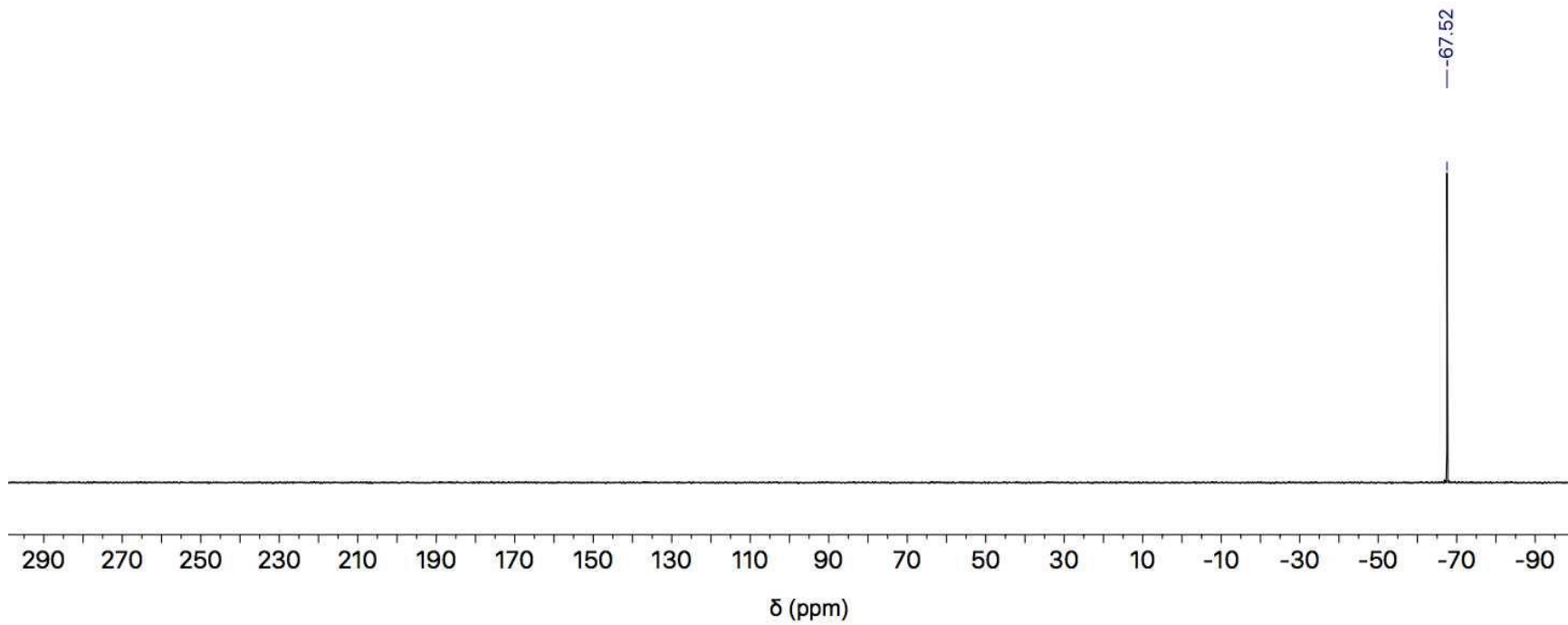
Figure S18. $^{31}P\{^1H\}$ NMR spectrum of **1•[H]₂**.
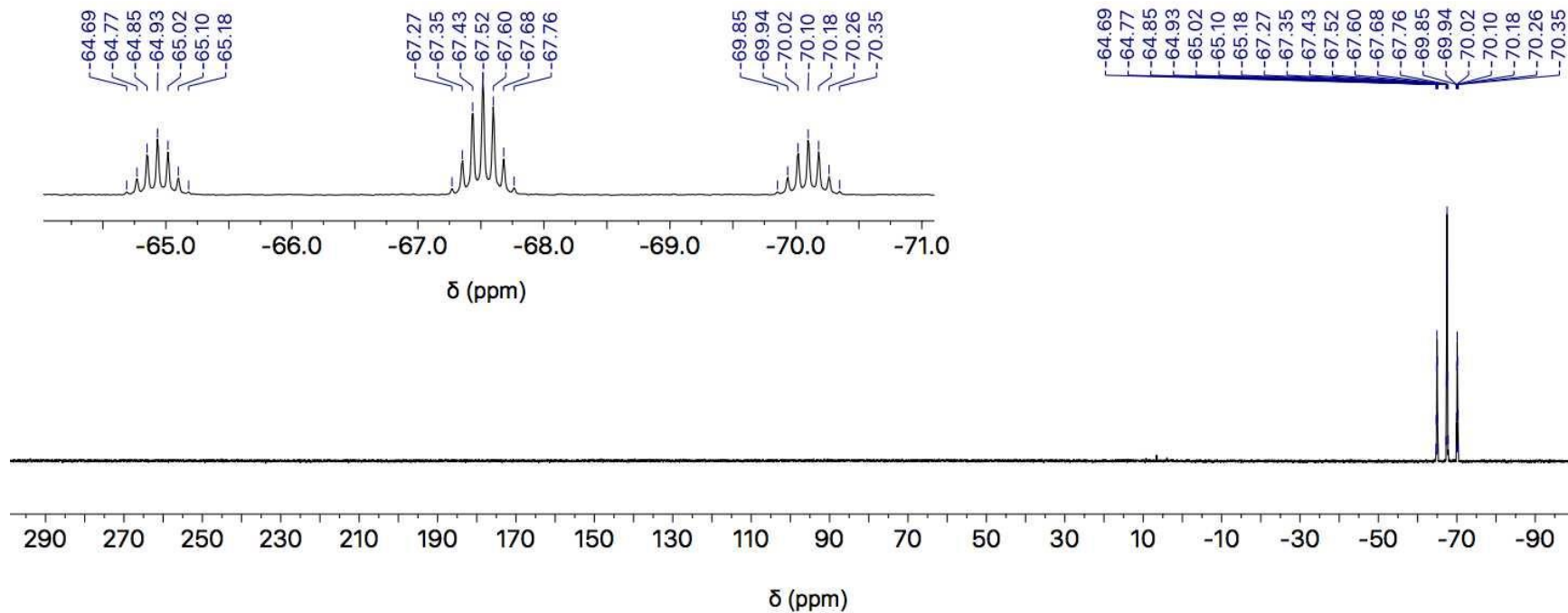
Figure S19. ^{31}P NMR spectrum of **1•[H]₂**.

VII. References

1. Pangborn, A. B.; Giardello, M. A.; Grubbs, R. H.; Rosen, R. K.; Timmers, F. J. Safe and Convenient Procedure for Solvent Purification. *Organometallics*, **1996**, *15*, 1518–1520.

2. Alaimo, P. J.; Peters, D. W.; Arnold, J.; Bergman, R. G. Suggested Modifications to a Distillation-Free Solvent Purification System. *J. Chem. Educ.*, **2001**, *78*, 64.

3. Bruker, *SAINT*, 2012, Bruker AXS Inc., Madison, Wisconsin, USA.

4. Bruker, *SADABS,* 2001, Bruker AXS Inc., Madison, Wisconsin, USA.

5. Sheldrick, G. M. A Short History of SHELX. *Acta. Cryst.*, **2008**, *A64*, 112-122.

6. Rydon, H.N.; Tonge, B.L. The Organic Chemistry of Phosphorus. Part VI. Some Phosphorus-containing Derivatives of 2,2,2-Trichloroethanol and N-Methylaniline. *J. Chem. Soc.* **1957**, 4862.

7. Zhao, W.; McCarthy, S. M.; Lai, T. Y.; Yennawar, H. P.; Radosevich, A. T. Reversible Intermolecular E–H Oxidative Addition to a Geometrically Deformed and Structurally Dynamic Phosphorous Triamide. *J. Am. Chem. Soc.* **2014**, *136*, 17634–17644.

8   Tanushi, A.; Radosevich, A.T. Insertion of a Nontrigonal Phosphorus Ligand into a Transition Metal-Hydride: Direct Access to a Metallohydrophosphorane. *J. Am. Chem. Soc.* **2018**, *140*, 8114-8118.

9. Trans, D.; Addison, A. W.; Rao, T. N. Synthesis, Structure, and Spectroscopic Properties of Copper(11) Compounds Containing Nitrogen-Sulphur Donor Ligands ; the Crystal and Molecular Structure of Aqua[l,7-Bis(N-Methylbenzimidazol-2'-Yl)- 2,6-Dithiaheptane]Copper(II) Perchlorate. *J. Chem. Soc. Dalton. Trans.* **1984**, 1349.

10. Solomon, E. I.; Hedman, B.; Hodgson, K. O.; Dey, A.; Szilagyi, R. K. Ligand K-edge X-ray Absorption Spectroscopy: Covalency of Ligand-Metal Bonds. *Coord. Chem. Rev.* **2005**, *249*, 97-129.

11. MacMillan, S. N.; Lancaster, K. M. X-ray Spectroscopic Interrogation of Transition-Metal-Mediated Homogeneous Catalysis: Primer and Case Studies. *ACS Catal.* **2017**, *7*, 1776-1791.

12. Donahue, C. M.; Daly, S. R. Ligand K-edge XAS Studies of Metal-Phosphorus Bonds: Applications, Limitations, and Opportunities. *Comments Inorg. Chem.* **2018**, *38*, 54-78.

13. Adhikari, D.; Mossin, S.; Basuli, F.; Huffman, J. C.; Szilagyi, R. K.; Meyer, K.; Mindiola, D. J. Structural, spectroscopic, and theoretical elucidation of a redox-active pincer-type ancillary applied in catalysis. *J. Am. Chem. Soc.* **2008**, *130*, 3676-3682.

14. Harkins, S. B.; Mankad, N. P.; Miller, A. J. M.; Szilagyi, R. K.; Peters, J. C. Probing the Electronic Structures of [Cu2(μ-XR2)]n+ Diamond Cores as a Function of the Bridging X Atom (X = N or P) and Charge (n = 0, 1, 2). *J. Am. Chem. Soc.* **2008**, *130*, 3478-3485.

15. Mankad, N. P.; Antholine, W. E.; Szilagyi, R. K.; Peters, J. C. Three-Coordinate Copper(I) Amido and Aminyl Radical Complexes. *J. Am. Chem. Soc.* **2009**, *131*, 3878-3880.

16. Mossin, S.; Tran, B. L.; Adhikari, D.; Pink, M.; Heinemann, F. W.; Sutter, J.; Szilagyi, R. K.; Meyer, K.; Mindiola, D. J. A Mononuclear Fe(III) Single Molecule Magnet with a 3/2↔5/2 Spin Crossover. *J. Am. Chem. Soc.* **2012**, *134*, 13651-13661.

17. Donahue, C. M.; McCollum, S. P.; Forrest, C. M.; Blake, A. V.; Bellott, B. J.; Keith, J. M.; Daly, S. R. Impact of Coordination Geometry, Bite Angle, and Trans Influence on Metal–Ligand Covalency in Phenyl-Substituted Phosphine Complexes of Ni and Pd. *Inorg. Chem.* **2015**, *54*, 5646-5659.

18. Lee, K.; Wei, H.; Blake, A. V.; Donahue, C. M.; Keith, J. M.; Daly, S. R. Ligand K-edge XAS, DFT, and TDDFT Analysis of Pincer Linker Variations in Rh(I) PNP Complexes: Reactivity Insights from Electronic Structure. *Dalton Trans.* **2016**, *45*, 9774-9785.

19. Blake, A. V.; Wei, H.; Lee, K.; Donahue, C. M.; Keith, J. M.; Daly, S. R. Solution and Solid Ligand K-edge XAS Studies of PdCl$_2$ Diphosphine Complexes with Phenyl and Cyclohexyl Substituents. *Eur. J. Inorg. Chem.* **2018**, 2267-2276.

20. Lee, K.; Wei, H.; Blake, A. V.; Donahue, C. M; Keith, J. M.; Daly, S. R. Measurement of Diphosphine σ-Donor and π-Acceptor Properties in d^0 Titanium Complexes Using Ligand K-edge XAS and TDDFT. *Inorg. Chem.* **2018**, *57,* 10277-10286.

21 Lee, K.; Wei, H.; Blake, A. V.; Donahue, C. M.; Keith, J. M.; Daly, S. R. Ligand K-edge XAS, DFT, and TDDFT Analysis of Pincer Linker Variations in Rh(I) PNP Complexes: Reactivity Insights from Electronic Structure. *Dalton Trans.* **2016**, *45*, 9774-9785.

22 Blake, A. V.; Wei, H.; Lee, K.; Donahue, C. M.; Keith, J. M.; Daly, S. R. Solution and Solid Ligand K-edge XAS Studies of PdCl$_2$ Diphosphine Complexes with Phenyl and Cyclohexyl Substituents. *Eur. J. Inorg. Chem.* **2018**, 2267-2276.

23. Blake, A. V.; Wei, H.; Donahue, C. M.; Lee, K.; Keith, J. M.; Daly, S. R. Solid Energy Calibration Standards for P K-edge XANES: Electronic Structure Analysis of PPh$_4$Br. *J. Synchrotron Radiat.* **2018**, *25*, 529-536.

24 Minasian, S. G.; Keith, J. M.; Batista, E. R.; Boland, K. S.; Kozimor, S. A.; Martin, R. L.; Shuh, D. K.; Tyliszczak, T.; Vernon, L. J. Carbon K-Edge X-ray Absorption Spectroscopy and Time-Dependent Density Functional Theory Examination of Metal-Carbon Bonding in Metallocene Dichlorides. *J. Am. Chem. Soc.* **2013**, *135*, 14731-14740.

25. Ravel, B.; Newville, M. ATHENA, ARTEMIS, HEPHAESTUS: data analysis for x-ray absorption spectroscopy using IFEFFIT. *J. Synchrotron Radiat.* **2005**, *12*, 537-541.

26. It is worth noting the contrast between the *C$_3$* molecular symmetry of P(NMePh)$_3$ and the *C$_s$* molecular symmetry of the related homoleptic triamide P(NMe$_2$)$_3$, see: Mitzel, N. W.; Smart, B. A.; Dreihäupl, K.-H.; Rankin, D. W. H.; Schmidbaur, H. Low Symmetry in P(NR$_2$)$_3$ Skeletons and Related Fragments: An Inherent Phenomenon. *J. Am. Chem. Soc.* **1996**, *118*, 12673–12682.

27. Gaussian 09, Revision B.01, Frisch, M.J.; Trucks, G.W.; Schlegel, H.B.; Scuseria, G.E.; Robb, M.A.; Cheeseman, J.R.; Scalmani, G.; Barone, V.; Mennucci, B.; Petersson, G.A.; Nakatsuji, H.; Caricato, M.; Li,X.; Hratchian, H.P.; Izmaylov, A.F.; Bloino, J.; Zheng, G.; Sonnenberg, J.L.; Hada, M.; Ehara, M.; Toyota, K.; Fukuda, R.; Hasegawa, J.; Ishida, M.; Nakajima, T.; Honda, Y.; Kitao, O.; Nakai, H.; Vreven, T.; Montgomery, J.A., Jr.; Peralta, J.E.; Ogliaro, F.; Bearpark, M.; Heyd, J.J.; Brothers, E.; Kudin, K.N.; Staroverov, V.N.; Kobayashi, R.; Normand, J.; Raghavachari, K.; Rendell, A.; Burant, J.C.; Iyengar, S.S.; Tomasi, J.; Cossi, M.; Rega, N.; Millam, N.J.; Klene, M.; Knox, J.E.; Cross, J.B.; Bakken, V.; Adamo, C.; Jaramillo, J.; Gomperts, R.; Stratmann, R.E.; Yazyev, O.; Austin, A.J.; Cammi, R.; Pomelli, C.; Ochterski, J. W.; Martin, R.L.; Morokuma, K.; Zakrzewski, V.G.; Voth, G.A.; Salvador, P.; Dannenberg, J.J.; Dapprich, S.; Daniels, A.D.; Farkas, Ö.; Foresman, J.B.; Ortiz, J.V.; Cioslowski, J.; Fox, D.J. Gaussian, Inc., Wallingford CT, 2009.

28. Becke, A. D. Density-Functional Thermochemistry. III. The Role of Exact Exchange. *J. Chem. Phys.* **1993**, *98*, 5648-5652.

29. Lee, C.; Yang, W.; Parr, R. G. Development of the Colle-Salvetti Correlation-Energy Formula into a Functional of the Electron Density. *Phys. Rev. B Condens. Matter* **1988**, *37*, 785-789.

30. Grimme, S.; Antony, J.; Ehrlich, S.; Krieg, H. A Consistent and Accurate Ab Initio Parametrization of Density Functional Dispersion Correction (DFT-D) for the 94 Elements H-Pu. *J. Chem. Phys.* **2010**, *132*, 154104/154101-154104/154119.

31. Hehre, W. J.; Ditchfield, R.; Pople, J. A. Self-Consistent Molecular Orbital Methods. XII. Further Extensions of Gaussian-Type Basis Sets for Use in Molecular Orbital Studies of Organic Molecules. *J. Chem. Phys.* **1972**, *56*, 2257-2261.

32. Hariharan, P. C.; Pople, J. A. Influence of Polarization Functions on MO Hydrogenation Energies. *Theor. Chim. Acta* **1973**, *28*, 213-222.

33. Hay, P. J.; Wadt, W. R. Ab Initio Effective Core Potentials for Molecular Calculations. Potentials for Potassium to Gold Including the Outermost Core Orbitals. *J. Chem. Phys.* **1985**, *82*, 299-310.

34. Roy, L. E.; Hay, P. J.; Martin, R. L. Revised Basis Sets for the LANL Effective Core Potentials. *J. Chem. Theory Comput.* **2008**, *4*, 1029-1031.

35. Ehlers, A. W.; Boehme, M.; Dapprich, S.; Gobbi, A.; Hoellwarth, A.; Jonas, V.; Koehler, K. F.; Stegmann, R.; Veldkamp, A.; et al. A Set of f-Polarization Functions for Pseudopotential Basis Sets of the Transition Metals Sc-Cu, Y-Ag and La-Au. *Chem. Phys. Lett.* **1993**, *208*, 111-114.

36. Martin, R. L. Natural Transition Orbitals. *J. Chem. Phys.* **2003**, *118*, 4775-4777.